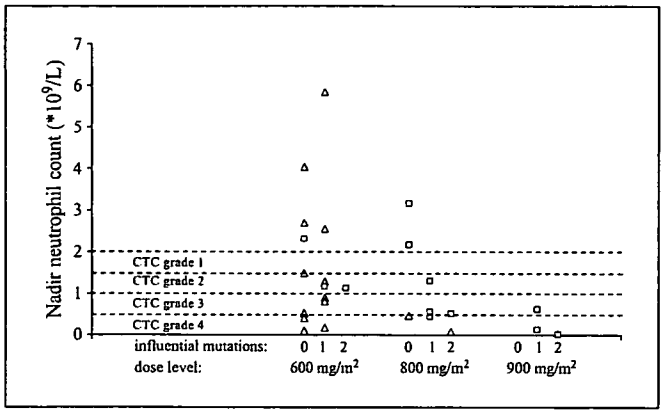

Fig. 2. Grade 4 neutropenia at cycle 1 was observed at dose levels 600, 800, and 900 mg/m^2. Nadir neutrophil counts of patients who were treated at these dose levels are plotted versus the number of influential mutations, i.e., the combined number of CYP2C9*3, CYP2C19*2, and CYP2C19*3 mutations. (△, Caucasian patients; □, Japanese patients).

for the various mutations could not adequately be determined using clinical data.

Simulation study of dose-limiting neutropenia. The hypothesis that CYP2C9*3, CYP2C19*2, and CYP2C19*3 polymorphisms may cause a higher risk of dose-limiting neutropenia was confirmed by the results of the simulation study listed in Table 4. These results show that the risk of dose-limiting neutropenia was increased by 40% or more in simulated patient groups with a single polymorphism. Homozygous mutations or combinations of multiple heterozygous mutations may result in a relative risk of serious toxicity of more than 2.

Dose adaptation. The CYP2C19*2 and CYP2C19*3 mutations caused a larger increase of the risk of dose-limiting neutropenia than CYP2C9*3. Consequently, the dosage of indisulam should be adapted to a larger extent for CYP2C19*2 and CYP2C19*3 than for CYP2C9*3. Each CYP2C19 mutation required a dose reduction of 100 mg/m^2. The recommended dose reduction for a CYP2C9*3 mutation was 50 mg/m^2. A simulation study showed that this guidance for dose adaptation resulted in the normalization of the relative risk of severe neutropenia (Table 4).

Discussion

In the current study, the relationships between various polymorphisms of two CYP450 enzymes (CYP2C9 and CYP2C19) and the pharmacokinetics of indisulam were assessed. It was shown that the elimination rate of indisulam was significantly decreased by CYP2C9*3, CYP2C19*2, and CYP2C19*3 polymorphisms. These CYP2C mutations caused an increased risk of dose-limiting neutropenia.

The activity of the *3-mutated CYP2C9 enzyme was shown to be reduced for *S*-warfarin *in vitro* by Haining et al. (33). This polymorphism was also associated to poor tolbutamide metabolism *in vivo* (34). In the current pharmacogenetic study, the *3 mutation in the CYP2C9 gene reduced the Michaelis-Menten elimination rate of indisulam. Thus, the saturable elimination pathway may correspond to hydroxylation of indisulam by CYP2C9 (19).

De Morais et al. (23, 24) showed that the *2 and *3 mutations in the CYP2C19 gene created a premature stop codon, resulting in a truncated nonfunctional CYP2C19 protein. These CYP2C19 mutations were related to poor metabolism of the CYP2C19 substrate (*S*)-mephenytoin (23, 24) and to a reduction of the clearance of indisulam. Consequently, the linear elimination pathway of indisulam may represent hydroxylation by CYP2C19 (19).

The CYP2C9*5 mutation results in lower enzymatic activity and that CYP2C19*4 represents a defective allele (30, 35). Therefore, the CYP2C9*5 and CYP2C19*4 polymorphisms may be related to reduced indisulam clearance. The AUC of indisulam in a patient who was heterozygous for the CYP2C9*5 mutation was indeed substantially higher than the AUC of three Caucasian wild-type patients who had received the same indisulam dose. Due to low allelic frequency, statistical significance of the effects of the CYP2C9*5 and CYP2C19*4 polymorphisms could not be shown in the present study.

In our population of Japanese and Caucasian patients, six CYP2C polymorphisms were observed, which are located on chromosome 10. The occurrence of multiple polymorphisms on the same allele is indicated by the haplotype. Multiple polymorphisms may not be fully independent. It may therefore be preferable to consider the haplotype rather than the genotype of individual polymorphisms for data analysis. This

Table 4. Simulated relative risk of dose-limiting neutropenia after administration of indisulam in a 1-h infusion and the 95% confidence intervals (in brackets)

Polymorphism	Caucasian heterozygous	Homozygous	Japanese heterozygous	Homozygous
Standard dose: 700 mg/m^2				
CYP2C9*3	1.39 (1.21-1.77)	2.24 (1.45-3.27)	1.47 (1.11-1.60)	NA
CYP2C19*2	1.86 (1.69-2.08)	NA	1.97 (1.73-2.33)	4.51 (3.31-6.25)
CYP2C19*3				
Adjusted dose: 700 mg/m^2—recommended dose reduction				
CYP2C9*3	1.03 (0.82-1.29)	1.30 (0.81-2.18)	1.09 (0.79-1.24)	NA
CYP2C19*2	1.04 (0.78-1.06)	NA	1.07 (0.86-1.20)	1.01 (0.69-1.62)
CYP2C19*3				

NOTE: Each subpopulation consisted of at least 10,000 simulated patients. These genotypes were not observed in the study population.
Abbreviation: NA, not applicable.

strategy was, however, not suitable for the current analysis because haplotype frequencies were too low.

The CYP2C19 polymorphisms occurred at much higher frequencies in the Japanese population compared with the Caucasian population (CYP2C19*2: 36% versus 9.8%; CYP2C19*3: 7.1% versus 0%). Because these CYP2C19 variants significantly impaired indisulam clearance, Japanese patients typically have a lower CL than Caucasians. Indeed, in the previously published population pharmacokinetic model, Japanese patients had a 3.4-fold lower value for CL than Caucasian individuals (16). This difference was not statistically significant upon inclusion of CYP2C19 genotype in the drug elimination model. This confirms that the lower linear clearance of indisulam in Japanese patients is due to genomic differences between the Caucasian and Japanese patient populations.

Mixed-effects modeling was used to assess the effects of CYP2C mutations on pharmacokinetic parameters. From a statistical standpoint, this method is superior to more commonly used methods in pharmacogenetic studies, where standard pharmacokinetic two-stage analyses are followed by conventional statistical tests in order assess differences between genetic subgroups (36).

It was shown that CYP2C9*3, CYP2C19*2, and CYP2C19*3 mutations led to decreased indisulam clearance and increased drug exposure. A clear relationship has been established between indisulam pharmacokinetics and its dose-limiting toxicities, neutropenia and thrombocytopenia. Based on the results of the present pharmacogenetic study and a semi-physiologic pharmacokinetic-pharmacodynamic model, it was expected that the risk of hematologic side effects is higher for patients with variant CYP2C9 and/or CYP2C19 alleles than for wild-type patients. A simulation study showed that the relative risk of dose-limiting neutropenia may be 2.2 for a homozygous Caucasian CYP2C9*3 mutant and 4.5 for a homozygous Japanese CYP2C19*2 mutant after administration of the recommended dosage of 700 mg/m^2 indisulam. Patient groups in the study population were too small to verify these estimated relative risks of dose-limiting neutropenia with observed data on hematologic toxicity. Nevertheless, the current clinical data imply that the CYP2C9*3 polymorphism is predictive for the occurrence of hematologic toxicity: the relative risk of grade 4 neutropenia was 2 in a group of 12 patients who were treated at the 600 mg/m^2 dose level and a patient with a homozygous CYP2C9*3 genotype had more severe neutropenia than a wild-type patient after administration of 800 mg/m^2. Furthermore, the lowest neutrophil nadir was observed in a Japanese homozygous CYP2C19*2 mutant patient.

The pharmacogenetic effects may be relevant for the treatment of patients with indisulam. Pretreatment genetic screening will permit planning of appropriate initial dosing for individual patients to achieve an optimal therapeutic effect. A reduced initial dosage for patients with high-risk CYP2C mutations is recommended. This recommendation is based on a retrospective study of limited sample size and should therefore be carefully interpreted. Haplotype frequencies in the study population were insufficient to provide a dosing strategy for patients with variant alleles of both CYP2C9 and CYP2C19.

In conclusion, CYP2C9*3, CYP2C19*2, and CYP2C19*3 polymorphisms were related to a decreased elimination rate of indisulam. Screening for these CYP2C polymorphisms may assist in the selection of an optimized initial indisulam dosage. It seems warranted to perform a prospective study to define solid recommendations for pharmacogenetically guided dose adjustments.

Acknowledgments

We thank Sanae Yasuda for her critical review of the manuscript.

References

1. Fukuoka K, Usuda J, Iwamoto Y, et al. Mechanisms of action of the novel sulfonamide anticancer agent E7070 on cell cycle progression in human non – small cell lung cancer cells. Invest New Drugs 2001;19: 219–27.
2. van Kesteren C, Beijnen JH, Schellens JHM. E7070: a novel synthetic sulfonamide targeting the cell cycle progression for the treatment of cancer. Anticancer Drugs 2002;13:989–97.
3. Haddad RI, Weinstein LJ, Wieczorek TJ, et al. A phase II clinical and pharmacodynamic study of E7070 in patients with metastatic, recurrent, or refractory squamous cell carcinoma of the head and neck: modulation of retinoblastoma protein phosphorylation by a novel chloroindolyl sulfonamide cell cycle inhibitor. Clin Cancer Res 2004;10:4680–7.
4. Raftopoulos H, Escudier B, Renshaw G, et al.: A phase II multicenter study of the cyclin-dependent kinase inhibitor indisulam in patients with inoperable and/or metastatic renal cell carcinoma (RCC) [abstract]. J Clin Oncol – American Society of Clinical Oncology Annual Meeting Proceedings (Post-Meeting Edition) 2004;22:414s.
5. Smyth JF, Aamdal S, Awada A, et al. Phase II study of E7070 in patients with metastatic melanoma. Ann Oncol 2005;16:158–61.
6. Fumoleau P, Viens P, Cottu PH, et al. A multi center phase II study of E7070, a chloroindolyl-sulfonamide anticancer agent in anthracycline and taxane pre treated breast cancer [abstract]. 26th San Antonio Breast Cancer Symposium 2003.
7. Talbot DC, Norbury C, Slade M, et al. A phase II and pharmacodynamic study of E7070 in patients with non – small cell lung cancer (NSCLC) who have failed platinum-based chemotherapy [abstract]. Proc Am Soc Clin Oncol 2002;21:327a.
8. Mainwaring PN, Van Cutsem E, Van Laethem JL, et al. A multicentre randomised phase II study of E7070 in patients with colorectal cancer who have failed 5-fluorouracil – based chemotherapy [abstract]. Proc Am Soc Clin Oncol 2002;21:153a.
9. Raymond E, ten Bokkel Huinink WW, Taieb J, et al. Phase I and pharmacokinetic study of E7070, a novel chloroindolyl sulfonamide cell-cycle inhibitor, administered as a one-hour infusion every three weeks in patients with advanced cancer. J Clin Oncol 2002; 20:3508–21.
10. Punt CJA, Fumoleau P, van de Walle B, Faber MN, Ravic M, Campone M. Phase I and pharmacokinetic study of E7070, a novel sulfonamide, given at a daily times five schedule in patients with solid tumors. A study by the EORTC-early clinical studies group (ECSG). Ann Oncol 2001;12:1289–93.
11. Terret C, Zanetta S, Roche H, et al. Phase I clinical and pharmacokinetic study of E7070, a novel sulfonamide given as a 5-day continuous infusion repeated every 3 weeks in patients with solid tumours. A study by the EORTC Early Clinical Study Group (ECSG). Eur J Cancer 2003;39:1097–104.
12. Dittrich C, Dumez H, Calvert H, et al. Phase I and pharmacokinetic study of E7070, a chloroindolyl-sulfonamide anticancer agent, administered on a weekly schedule to patients with solid tumors. Clin Cancer Res 2003;9:5195–204.
13. Raymond E, Fumoleau P, Roche H, et al. Combined results of 4 phase I and pharmacokinetic studies of E7070, a novel chloroindoly-sulphonamide inhibiting the activation of cdk2 and cyclin E [abstract]. Clin Cancer Res 2000;6:4529s.
14. Yamada Y, Yamamoto N, Shimoyama T, et al. Phase I pharmacokinetic and pharmacogenomic study of E7070 administered once every 21 days. Cancer Sci 2005;96:721–8.
15. van Kesteren C, Mathôt RAA, Raymond E, et al. Population pharmacokinetics of the novel anticancer agent E7070 during four phase I studies: model building and validation. J Clin Oncol 2002;20: 4065–73.
16. Zandvliet AS, Schellens JHM, Copalu W, Beijnen JH, Huitema ADR. A semi-physiological population pharmacokinetic model describing the non-linear disposition of indisulam. J Pharmacokinet Pharmacodyn 2006;33:543–70.
17. van Kesteren C, Zandvliet AS, Karlsson MO, et al. Semi-physiological model describing the hematological toxicity of the anti-cancer agent indisulam. Invest New Drugs 2005;23:225–34.
18. van den Bongard HJGD, Pluim D, Rosing H, et al. An excretion balance and pharmacokinetic study of the novel anticancer agent E7070 in cancer patients. Anticancer Drugs 2002;13:807–14.
19. Beumer JH, Hillebrand MJX, Pluim D, et al. Human metabolism of [(14)C]indisulam following i.v.

infusion in cancer patients. Invest New Drugs 2005; 23:317–30.
20. Rodrigues AD. Integrated cytochrome P450 reaction phenotyping: attempting to bridge the gap between cDNA-expressed cytochromes P450 and native human liver microsomes. Biochem Pharmacol 1999;57:465–80.
21. Beumer JH, Rosing H, Hillebrand MJX, et al. Quantitative determination of the novel anticancer drug E7070 (indisulam) and its metabolite (1,4-benzene disulphonamide) in human plasma, urine and faeces by high-performance liquid chromatography coupled with electrospray ionization tandem mass spectrometry. Rapid Commun Mass Spectrom 2004;18:2839–48.
22. U.S. Department of Health and Human Services, Food and Drug Administration, Center for Drug Evaluation and Research (CDER). Guidance for Industry: Bioanalytical Method Validation. 2001.
23. De Morais SM, Wilkinson GR, Blaisdell J, Meyer UA, Nakamura K, Goldstein JA. Identification of a new genetic defect responsible for the polymorphism of (*S*)-mephenytoin metabolism in Japanese. Mol Pharmacol 1994;46:594–8.
24. De Morais SM, Wilkinson GR, Blaisdell J, Nakamura K, Meyer UA, Goldstein JA. The major genetic defect responsible for the polymorphism of *S*-mephenytoin metabolism in humans. J Biol Chem 1994;269: 15419–22.
25. Xie HG, Prasad HC, Kim RB, Stein CM. CYP2C9 allelic variants: ethnic distribution and functional significance. Adv Drug Deliv Rev 2002;54:1257–70.
26. Allabi AC, Gala JL, Desager JP, Heusterspreute M, Horsmans Y. Genetic polymorphisms of CYP2C9 and CYP2C19 in the Beninese and Belgian populations. Br J Clin Pharmacol 2003;56:653–7.
27. Kidd RS, Curry TB, Gallagher S, Edeki T, Blaisdell J, Goldstein JA. Identification of a null allele of CYP2C9 in an African-American exhibiting toxicity to phenytoin. Pharmacogenetics 2001;11:803–8.
28. Xie HG, Stein CM, Kim RB, Wilkinson GR, Flockhart DA, Wood AJ. Allelic, genotypic and phenotypic distributions of *S*-mephenytoin 4′-hydroxylase (CYP2C19) in healthy Caucasian populations of European descent throughout the world. Pharmacogenetics 1999;9: 539–49.
29. Goldstein JA, Ishizaki T, Chiba K, et al. Frequencies of the defective CYP2C19 alleles responsible for the mephenytoin poor metabolizer phenotype in various Oriental, Caucasian, Saudi Arabian and American black populations. Pharmacogenetics 1997;7:59–64.
30. Ferguson RJ, De Morais SM, Benhamou S, et al. A new genetic defect in human CYP2C19: mutation of the initiation codon is responsible for poor metabolism of *S*-mephenytoin. J Pharmacol Exp Ther 1998;284: 356–61.
31. Xiao ZS, Goldstein JA, Xie HG, et al. Differences in the incidence of the CYP2C19 polymorphism affecting the *S*-mephenytoin phenotype in Chinese Han and Bai populations and identification of a new rare CYP2C19 mutant allele. J Pharmacol Exp Ther 1997; 281:604–9.
32. Ibeanu GC, Goldstein JA, Meyer U, et al. Identification of new human CYP2C19 alleles (CYP2C19*6 and CYP2C19*2B) in a Caucasian poor metabolizer of mephenytoin. J Pharmacol Exp Ther 1998;286: 1490–5.
33. Haining RL, Hunter AP, Veronese ME, Trager WF, Rettie AE. Allelic variants of human cytochrome P450 2C9: baculovirus-mediated expression, purification, structural characterization, substrate stereoselectivity, and prochiral selectivity of the wild-type and I359L mutant forms. Arch Biochem Biophys 1996;333: 447–58.
34. Sullivan-Klose TH, Ghanayem BI, Bell DA, et al. The role of the CYP2C9–359 allelic variant in the tolbutamide polymorphism. Pharmacogenetics 1996;6: 341–9.
35. Dickmann LJ, Rettie AE, Kneller MB, et al. Identification and functional characterization of a new CYP2C9 variant (CYP2C9*5) expressed among African Americans. Mol Pharmacol 2001;60:382–7.
36. Ette EI, Williams PJ. Population pharmacokinetics I: background, concepts, and models. Ann Pharmacother 2004;38:1702–6.

AZD2171 Shows Potent Antitumor Activity Against Gastric Cancer Over-Expressing Fibroblast Growth Factor Receptor 2/Keratinocyte Growth Factor Receptor

Masayuki Takeda,[1,3] Tokuzo Arao,[1,4] Hideyuki Yokote,[1,4] Teruo Komatsu,[5] Kazuyoshi Yanagihara,[5] Hiroki Sasaki,[6] Yasuhide Yamada,[2] Tomohide Tamura,[2] Kazuya Fukuoka,[7] Hiroshi Kimura,[3] Nagahiro Saijo,[2] and Kazuto Nishio[1,4]

Abstract

Purpose: AZD2171 is an oral, highly potent, and selective vascular endothelial growth factor signaling inhibitor that inhibits all vascular endothelial growth factor receptor tyrosine kinases. The purpose of this study was to investigate the activity of AZD2171 in gastric cancer.

Experimental Design: We examined the antitumor effect of AZD2171 on the eight gastric cancer cell lines *in vitro* and *in vivo*.

Results: AZD2171 directly inhibited the growth of two gastric cancer cell lines (KATO-III and OCUM2M), with an IC_{50} of 0.15 and 0.37 μmol/L, respectively, more potently than the epidermal growth factor receptor tyrosine kinase inhibitor gefitinib. Reverse transcription-PCR experiments and immunoblotting revealed that sensitive cell lines dominantly expressed COOH terminus–truncated fibroblast growth factor receptor 2 (FGFR2) splicing variants that were constitutively phosphorylated and spontaneously dimerized. AZD2171 completely inhibited the phosphorylation of FGFR2 and downstream signaling proteins (FRS2, AKT, and mitogen-activated protein kinase) in sensitive cell lines at a 10-fold lower concentration (0.1 μmol/L) than in the other cell lines. An *in vitro* kinase assay showed that AZD2171 inhibited kinase activity of immunoprecipitated FGFR2 with submicromolar K_i values (~0.05 μmol/L). Finally, we assessed the antitumor activity of AZD2171 in human gastric tumor xenograft models in mice. Oral administration of AZD2171 (1.5 or 6 mg/kg/d) significantly and dose-dependently inhibited tumor growth in mice bearing KATO-III and OCUM2M tumor xenografts.

Conclusions: AZD2171 exerted potent antitumor activity against gastric cancer xenografts over-expressing FGFR2. The results of these preclinical studies indicate that AZD2171 may provide clinical benefit in patients with certain types of gastric cancer.

Various anticancer therapies for gastric cancer have been investigated over the past two decades. Despite intensive studies, the prognosis for patients with unresectable advanced or recurrent gastric cancer remains poor (1, 2), and new therapeutic modalities are needed.

Authors' Affiliations: [1]Shien Lab and [2]Medical Oncology, National Cancer Center Hospital, Tsukiji, Chuo-ku, Tokyo, Japan; [3]Second Department of Internal Medicine, Nara Medical University; [4]Department of Genome Biology, Kinki University School of Medicine, Ohno-higashi, Osaka-Sayama, Osaka, Japan; and [5]Central Animal Lab and [6]Genetic Division, National Cancer Center Research Institute; and [7]Division of Respiratory Medicine, Department of Internal Medicine, Hyogo College of Medicine, Nishinomiya, Hyogo, Japan

Received 11/16/06; revised 1/29/07; accepted 2/27/07.

Grant support: Third-Term Comprehensive 10-Year Strategy for Cancer Control and program for promotion of Fundamental Studies in Health Sciences of the National Institute of Biomedical Innovation and Japan Health Sciences Foundation. The costs of publication of this article were defrayed in part by the payment of page charges. This article must therefore be hereby marked *advertisement* in accordance with 18 U.S.C. Section 1734 solely to indicate this fact.

Note: M. Takeda and T. Arao are the recipient of a Research Resident Fellowship from the Foundation of Promotion of Cancer Research in Japan.

Requests for reprints: Kazuto Nishio, Department of Genome Biology, Kinki University School of Medicine, 377-2 Ohno-higashi, Osaka-Sayama, Osaka 589-8511, Japan. Fax: 81-72-366-0206; E-mail: knishio@med.kindai.ac.jp.

©2007 American Association for Cancer Research.

doi:10.1158/1078-0432.CCR-06-2743

Fibroblast growth factors (FGF) and their signaling receptors have been found to be associated with multiple biological activities, including proliferation, differentiation, motility, and transforming activities (3–5). The *K-sam* gene was first identified as an amplified gene in human gastric cancer cell line KATO-III (6, 7), and its product was later found to be identical to the bacteria-expressed kinase, or keratinocyte growth factor receptor (KGFR), and FGF receptor 2 (FGFR2). FGFR2/KGFR/K-sam is preferentially amplified in poorly differentiated types of gastric cancers with a malignant phenotype, and its protein expression was detected by immunohistochemical staining from 20 of 38 cases of the undifferentiated type of advanced stomach cancer (8, 9). Thus, FGFR2 signaling may be as a promising molecular target for gastric cancer.

AZD2171 is a potent, ATP-competitive small molecule that inhibits all vascular endothelial growth factor receptors [VEGFR-1, VEGFR-2 (also known as KDR), and VEGFR-3]. *In vitro* studies have shown that recombinant VEGFR-2 tyrosine kinase activity was potently inhibited by AZD2171 (IC_{50} <1 nmol/L; ref. 10). AZD2171 also showed potent activity versus VEGFR-1 and VEGFR-3 (IC_{50}, 5 and ≤3 nmol/L, respectively). VEGF-stimulated proliferation and VEGFR-2 phosphorylation of human umbilical vascular endothelial cells

was inhibited by AZD2171 (IC_{50}, 0.4 and 0.5 nmol/L, respectively). In *in vivo* studies, inhibition of VEGFR-2 signaling by AZD2171 reduced microvessel density and dose-dependently inhibited the growth of various human tumor xenografts (colon, lung, prostate, breast, and ovary; ref. 10). These data are consistent with potent inhibition of VEGF signaling, angiogenesis, neovascular survival, and tumor growth. On the other hand, because it was known that AZD2171 also possesses additional activity against FGFR1 (IC_{50}, 26 nmol/L; ref. 10), we hypothesized that AZD2171 may exhibit the additional anticancer activity against FGFR-overexpressing gastric cancer cells.

Our previous studies showed significant activities of the dual VEGFR-2 and epidermal growth factor receptor inhibitor ZD6474 against poorly differentiated gastric cancer (11) and non-small-cell lung cancer with epidermal growth factor receptor mutations (12, 13), both *in vitro* and *in vivo*. Based on these findings, we proceeded to investigate the anticancer activity of AZD2171 in preclinical models (gastric cell lines and xenografts).

Materials and Methods

Anticancer agents. AZD2171 and gefitinib (Iressa) were provided by AstraZeneca. AZD2171 and gefitinib were dissolved in DMSO for the *in vitro* experiments, and AZD2171 was suspended in 1% (w/v) aqueous polysorbate 80 and administered in a dose of 0.1 mL/10 g per body weight in the *in vivo* experiments.

Cell culture. Human gastric cancer cell lines 44As3, 58As1, OKAJIMA, OCUM2M, KATO-III, MKN-1, MKN-28, and MKN-74 were maintained in RPMI 1640 (Sigma) supplemented with 10% heat-inactivated fetal bovine serum (Life Technologies) and penicillin-streptomycin.

Established highly tumorigenic cell line. Signet ring cell gastric carcinoma cell line KATO-III was gift from Dr. M. Sekiguchi (University of Tokyo, Tokyo, Japan). All of the presented *in vitro* experiments were done using the KATOIII cell line. We conducted a preliminary experiment to compare the cellular characteristics of TU-KATO-III cells and KATOIII cells, and the results revealed that a high expression level of FGFR2 and high sensitivity to AZD2171 were still maintained in the TU-KATO-III cells (data not shown). KATO-III did not show tumorigenicity following repeated implantation of the cultured cells into BALB/c nude mice. Following s.c. inoculation into nonobese diabetic/severe combined immunodeficient mice, 80% to 100% of the KATO-III cells caused the formation of tumor. Following this result, we cultured the cancer cells isolated from the tumor of mice that developed 2 to 3 months following the implantation of KATO-III cells and attempted s.c. injection into nude mice, in turn, of the incubated cells. This sequence of manipulations was repeated for seven cycles in an attempt to reliably isolate cell lines that would have higher potential to undergo tumor formation over short periods of time. In this way, we obtained a cell line (TU-kato-III) from KATO-III cells that possessed a high tumorigenic potential.

In vitro *growth inhibition assay.* The 3-(4,5-dimethylthiazol-2-yl)-2,5-diphenyltetrazolium bromide assay was used to evaluate the growth-inhibitory effect of AZD2171. Cell suspensions (180 μL) were seeded into each well of 96-well microculture plate and incubated in 10% fetal bovine serum medium for 24 h. The cells were exposed to AZD2171 or gefitinib at concentrations ranging from 4 nmol/L to 80 μmol/L and cultured at 37°C in a humidified atmosphere for 72 h. After the culture period, 20 μL 3-(4,5-dimethylthiazol-2-yl)-2,5-diphenyltetrazolium bromide reagent was added, and the plates were incubated for 4 h. After centrifugation, the culture medium was discarded, and wells were filled with DMSO. The absorbance of the cultures at 562 nmol/L was measured using Delta-soft on a Macintosh computer (Apple) interfaced to a Bio-Tek Microplate Reader EL-340 (BioMatellics). This experiment was done in triplicate.

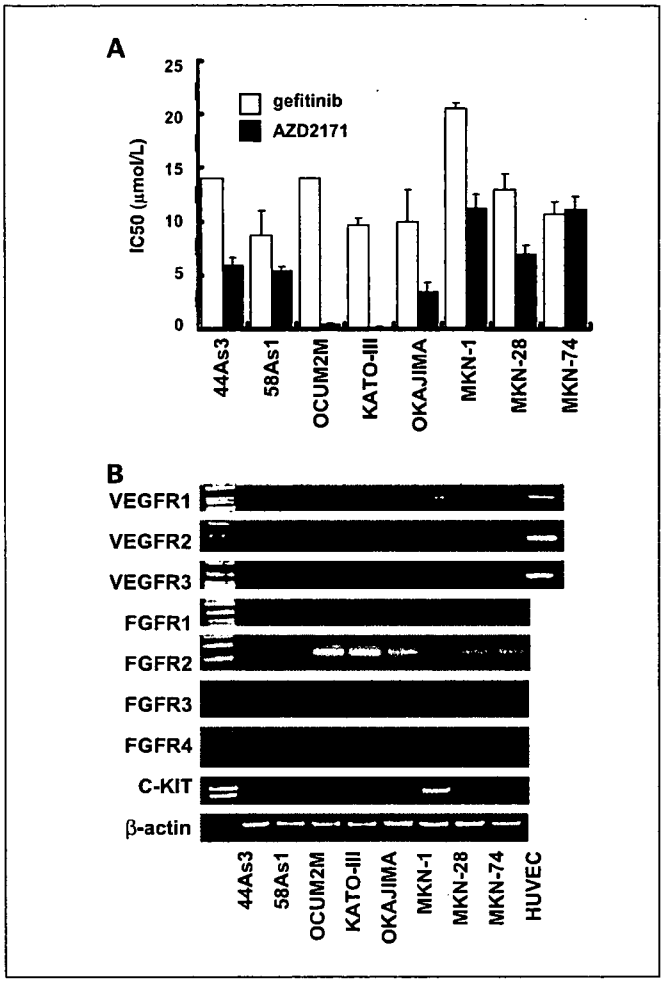

Fig. 1. *A, in vitro* growth-inhibitory effect of AZD2171 and gefitinib on eight gastric cancer cell lines. AZD2171 had a growth-inhibitory effect on KATO-III cells and OCUM2M cells (IC_{50}, 0.15 and 0.37 μmol/L, respectively). Columns, mean IC_{50} of each compound from three independent experiments; bars, SD. □, IC_{50} of gefitinib; ■, IC_{50} of AZD2171. *B,* the mRNA expression levels of VEGFRs, FGFRs, and c-KIT in gastric cancer cell lines were determined by reverse transcription-PCR. Human umbilical vascular endothelial cells were used as the positive control for the VEGFRs. No mRNA expression of VEGFRs or c-KIT was detected by reverse transcription-PCR in both sensitive cell lines, but FGFR2 was strongly detected; however, little faint or none was detected in the other cell lines.

Reverse-transcription PCR. Using a GeneAmp RNA-PCR kit (Applied Biosystems), 5 μg of total RNA from each cultured cell line was converted to cDNA. The PCR amplification procedure consisted of 28 to 35 cycles (95°C for 45 s, 62°C for 45 s, and 72°C for 60 s) followed by incubation at 72°C for 7 min, and the bands were visualized by ethidium bromide staining. The following primers were used for the PCR: human-specific β-actin, forward 5-GGAAATCGTGCGTGACATT-3 and reverse 5-CATCTGCTGGAAGGTGGACAG-3; VEGFR-1, forward 5-TAGCGTCACCAGCAGCGAAAGC-3 and reverse 5-CCTTTCTTTTGGGTCTCTGTGC-3; VEGFR-2, forward 5-CAGACGGACAGTGGTATGGTTC-3 and reverse 5-ACCTGCTGGTGGAAAGAACAAC-3; VEGFR-3, forward 5-AGCCATTCATCAACAAGCCT-3 and reverse 5-GGCAACAGCTGGATGTCATA-3; c-KIT, forward 5-GCCCACAATAGATTGGTATTT-3 and reverse 5-AGCATCTTTACAGCGACAGTC-3; FGFR1, forward 5-GGAGGATCGAGCTCACTCGTGG-3 and reverse

5-CGGAGAAGTAGGTGGTGTCAC-3; FGFR2, forward 5-CAGTAGGACTGTAGACAGTGAA-3 and reverse 5-CCGGTGAGGCGATCGCTCCACA-3; FGFR3, forward 5-GGTCAAGGATGGCACAGGGCTG-3 and reverse 5-AGCAGCTTCTTGTCCATCCGCT-3; and FGFR4, forward 5-CCGCCTAGAGATTGCCAGCTTC-3 and reverse 5-AGGCCTGTCCATCCTTAAGCCA-3.

Real-time reverse transcription-PCR. Real-time reverse transcription-PCR amplification was done by using a Premix Ex Taq and Smart Cycler system (Takara Bio, Inc.) according to the manufacturer's instructions. The following primers were used: FGFR2 (IIIb), forward 5-GATAAATAGTTCCAATGCAGAAGTGCT-3 and reverse 5-TGCCCTATATAATTGGAGACCTTACA-3 (7); FGFR2 (COOH-terminal), forward 5-GAATACTTGGACCTCAGCCAA-3 and reverse 5-AACACTGCCGTTTATGTGTGG-3; and human-specific β-actin, forward 5-GGAAATCGTGCGTGACATT-3 and reverse 5-CATCTGCTGGAAGGTGGACAG-3. The experiment was independently done in triplicate using β-actin as a reference to normalize the data.

Western blotting. Cells were cultured overnight in 10% serum-containing medium or serum-starved medium and exposed to 0.1 to 10 μmol/L of AZD2171 for 3 h before addition of KGF (100 ng/mL) for 15 min. Immunoblotting was done as described previously (14). In brief, after lysing the cells in radioimmunoprecipitation buffer, the lysate was electrophoresed through 10% (w/v) polyacrylamide gels. The proteins were transferred to polyvinylidene difluoride membranes and reacted with the following antibodies: anti-FGFR2 (H-80) and anti-FGFR2 (C-17) antibody (Santa Cruz Biotechnology, Inc.); anti-phosphotyrosine antibody PY20 (BD Transduction Laboratories); anti-phosphorylated FGFR (Tyr653/654), anti-mitogen-activated protein kinase, anti-phosphorylated mitogen-activated protein kinase antibody, anti-AKT, anti-phosphorylated AKT, and anti-rabbit horseradish peroxidase-conjugated antibody (Cell Signaling Technology); and anti-β-actin antibody (Sigma). Visualization was achieved with an enhanced chemiluminescent detection reagent (Amersham Bioscience).

FGFR2 kinase assay. FGFR2/KGFR kinase activity was quantified by using a Universal Tyrosine Kinase Assay kit (Takara) according to manufacturer's instructions. FGFR2/KGFR proteins were collected from the KATO-III, OCUM2M, and OKAJIMA cell lysates by overnight immunoprecipitation with an anti-FGFR2 antibody. The FGFR2/KGFR immune complexes were washed thrice with radioimmunoprecipitation assay buffer and diluted kinase reaction buffer. Immobilized tyrosine kinase substrate (poly[Glu-Tyr]) was incubated for 30 min at 37°C with each sample in the presence of kinase-reacting solution and ATP. Samples were washed four times, blocked with blocking solution, and incubated with anti-phosphotyrosine antibody (PY20) conjugated to horseradish peroxidase. The absorbance of the phosphorylated substrate was measured at 450 nm.

Chemical cross-link analysis. The chemical cross-link analysis was carried out as described previously (15). In brief, KATO-III cells and OKAJIMA cells were cultured under serum-starved conditions for 24 h, and after stimulation with KGF (100 ng/mL) for 15 min, they were collected and washed with PBS and incubated for 30 min in PBS

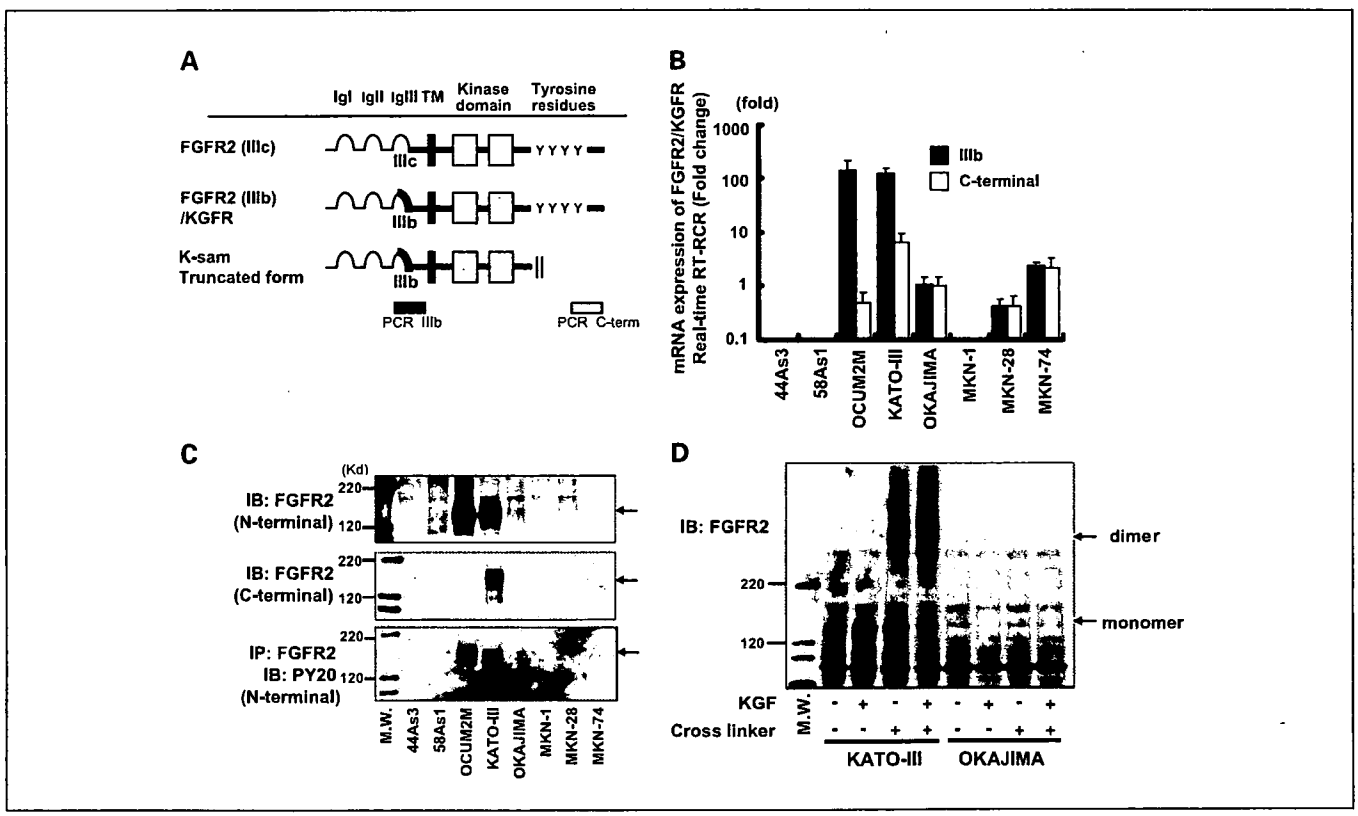

Fig. 2. *A*, schematic representation of FGFR2 and regions amplified by PCR. *B*, mRNA expression levels of FGFR2 were quantified by detecting the extracellular domain or COOH-terminal region by real-time reverse transcription-PCR. Expression in the cells is shown as a ratio to expression in OKAJIMA cells. FGFR2 was overexpressed in KATO-III cells and OCUM2M cells by about 100-fold compared with the other cell lines. The majority of the FGFR2 in the sensitive cell lines KATO-III and OCUM2M had no COOH-terminal region. *C*, protein expression levels of FGFR2 were determined by Western blotting with antibodies to the NH_2 or COOH termini. Both AZD2171-sensitive cell lines overexpressed FGFR2, and the phosphorylation levels were markedly higher. *D*, chemical cross-linking analysis. Cells were cultured under serum-starved conditions for 24 h and then stimulated with KGF (100 ng/mL) for 15 min. After collecting and washing them with PBS, they were incubated for 30 min in PBS containing cross-linker substrate. The reaction was terminated by adding 250 mmol/L glycine for 5 min. In spite of the serum-starved conditions, high levels of expression of the dimerized form were observed in KATO-III cells in the absence of ligand stimulation. This phenomenon was not observed in the control undifferentiated OKAJIMA cell line. Ligand stimulation resulted in a mild increase in the dimerized form in KATO-III cells. Arrows indicate monomer or dimer formation.

containing 1.5 mmol/L of the non-permeable cross-linker bis-(sulfosuccinimidyl) substrate (Pierce). The reaction was terminated by adding 250 mmol/L glycine for 5 min, and the cells were analyzed by immunoblotting with FGFR2 antibody (Sigma).

FGFR2/KGFR gene silencing with small interfering RNA. Predesigned small interfering RNA (siRNA) targeting FGFR2 was purchased from Ambion. KATO-III cells were plated on a 96-well plate and incubated in serum-containing medium for 24 h. The cells were then transfected with the FGFR2 targeting siRNA or non-silencing siRNA using RNAiFect Transfection Reagent (Qiagen) according to the manufacturer's protocol and incubated another 72 h. Cell growth was evaluated by the 3-(4,5-dimethylthiazol-2-yl)-2,5-diphenyltetrazolium bromide assay. For immunoblotting, 2×10^5 cells per well were plated on a six-well plate for 24 h and transfected with siRNA under the same conditions.

In vivo *experiments.* Tumorigenic TU-kato-III cells were derived from the gastric cancer cell line KATO-III. Four-week-old female BALB/c nude mice were purchased from CLEA Japan, Inc. and maintained under specific-pathogen-free conditions; 5×10^6 TU-kato-III cells or OCUM2M cells were s.c. injected into both flanks of each mouse. When the tumors had reached a volume of 0.1-0.3 cm^3, the mice were randomized into three groups (three per group) and given AZD2171, 1.5 or 6.0 mg/kg/d, or vehicle once daily by oral gavage for 3 weeks. Tumor volume was calculated using the formula: (length × width) × $\sqrt{}$(length × width) × (π/6), where length is the longest diameter across the tumor, and width is the corresponding perpendicular. All mice were sacrificed on day 21, and the tumors were collected. The protocol of the experiment was approved by the Committee for Ethics in Animal Experimentation and conducted in accordance with the Guidelines for Animal Experiments of National Cancer Center.

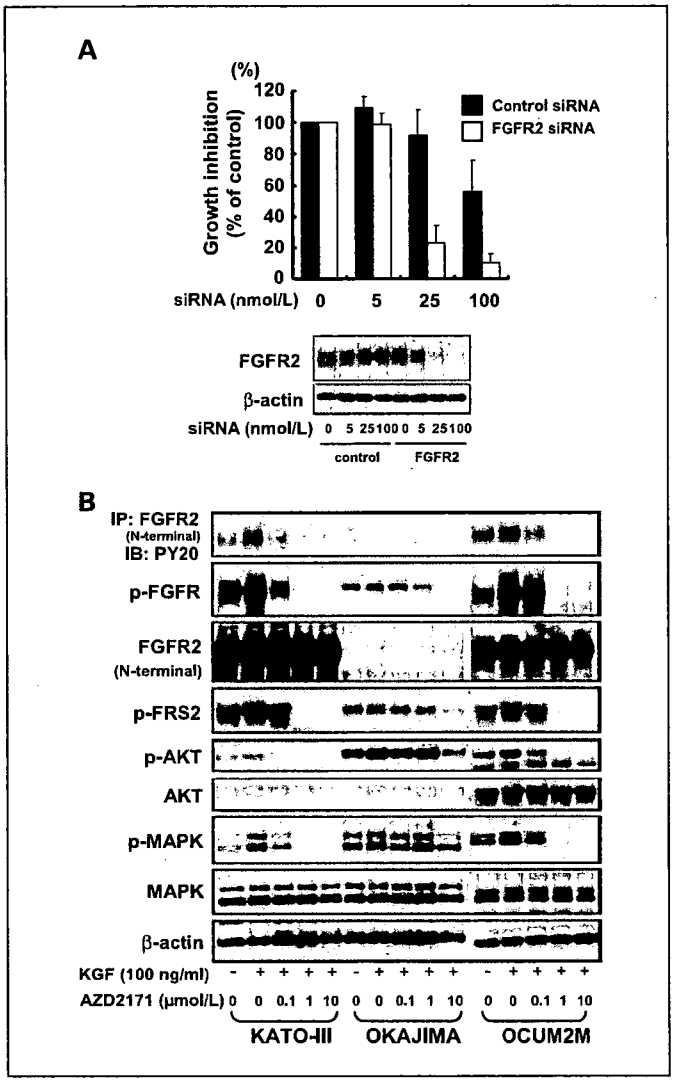

Fig. 3. *A,* FGFR2 targeting siRNA and cellular growth-inhibitory effect. KATO-III cells were plated on a 96-well plate and incubated in serum-containing medium for 24 h. After incubation, the cells were transfected with FGFR2-targeting or non-silencing siRNA and incubated for another 72 h. Cell growth was evaluated by 3-(4,5-dimethylthiazol-2-yl)-2,5-diphenyltetrazolium bromide assay. For immunoblotting, 2×10^5 cells per well were plated on a six-well plate and treated similarly. Marked inhibition of cell growth (−80%) was observed by FGFR2 targeting siRNA compared with control siRNA (*top*). Reduction of FGFR2 protein expression in KATO-III cells was confirmed by immunoblotting (*bottom*). Columns, % control absorbance in three independent experiments; bars, SD. *B,* Western blotting for downstream molecules of FGFR2 signaling. Cells were cultured overnight under serum-starved conditions and exposed to 0.1 to 10 μmol/L AZD2171 for 3 h before adding 100 ng/mL KGF for 15 min. AZD2171 completely inhibited KGF-induced phosphorylation of FGFR2 at 1 μmol/L in the sensitive cell lines, compared with 10 μmol/L in the control cell line OKAJIMA. Similar results were observed for FRS-2, AKT, and mitogen-activated protein kinase (*MAPK*).

Results

AZD2171 showed growth-inhibitory activity in vitro. To evaluate the growth-inhibitory activity of AZD2171 *in vitro*, we did 3-(4,5-dimethylthiazol-2-yl)-2,5-diphenyltetrazolium bromide assays on eight gastric cancer cell lines. The epidermal growth factor receptor–specific tyrosine kinase inhibitor gefitinib was used as a reference. The IC_{50} of gefitinib for all cell lines was between 7 and 20 μmol/L. AZD2171 inhibited the growth of KATO-III cells and OCUM2M cells (IC_{50}, 0.15 and 0.37 μmol/L, respectively) more potently than the other cell lines (Fig. 1A).

Expression levels of tyrosine kinase receptors. To elucidate the mechanism of action of AZD2171 in the two sensitive cell lines, we measured mRNA expression levels of VEGFRs, FGFRs, and c-KIT, whose kinase activity have been reported to be inhibited by AZD2171 (10). No mRNA expression of VEGFRs or c-KIT was detected by reverse transcription-PCR in either sensitive cell lines. FGFR2 transcripts, however, were strongly expressed in both sensitive cell lines but not strongly in the other cell lines (Fig. 1B). Since we previously found that FGFR2/KGFR/K-sam with a deletion of COOH-terminal exons was amplified in both sensitive cell lines (9), we speculated that amplified FGFR2/KGFR might be associated with sensitivity to AZD2171.

Sensitive cells expressed constitutively active and spontaneously dimerized FGFR2/KGFR. We quantified mRNA expression levels of FGFR2 by real-time reverse transcription-PCR with primers that detect the extracellular domain (IIIb region, see Fig. 2A) and COOH-terminal region. The results show that KATO-III cells and OCUM2M cells expressed FGFR2 100-fold higher than the other cells tested. The COOH-terminal region of FGFR2 was deleted in the KATO-III cells and OCUM2M cells (Fig. 2B). Overexpression and markedly increased phosphorylation of FGFR2 was observed in the AZD2171-sensitive cell lines (Fig. 2C).

Immunoblotting with antibodies for the COOH and NH_2 termini revealed that almost all the FGFR2 expressed by OCUM2M cells, and about half of FGFR2 expressed by KATO-III cells, were truncated (Fig. 2C). Although the KATO-III cells expressed wild-type receptor to some extent, the

Table 1. *In vitro* kinase assay of AZD2171 against FGFR2

Cell line	K_m	K_i (μmol/L)
KATO-III	8.3 ± 3.3	0.067 ± 0.017
OCUM2M	7.1 ± 1.4	0.072 ± 0.022
OKAJIMA	11.0 ± 5.0	0.049 ± 0.041

COOH-terminal truncated type was dominantly expressed in AZD2171-sensitive cell lines.

A chemical cross-linking analysis was done to evaluate the dimerization of FGFR2. High dimerization of FGFR2 was observed in the KATO-III cells even in the absence of ligand stimulation (Fig. 2D), but no such phenomenon was observed in the control undifferentiated OKAJIMA cell line. Ligand stimulation increased the level of the dimerized-form in KATO-III cells. Taken together, these findings show that the sensitive cell lines expressed high levels of FGFR2 that was highly phosphorylated and spontaneously dimerized without ligand stimulation, suggesting that FGFR2 signaling is constitutively activated in these cells. This evidence is consistent with the widely recognized findings that cancer cells sensitive to other tyrosine kinase inhibitors, such as gefitinib and imatinib, overexpress the highly phosphorylated target receptor with an increased level of dimerization in a ligand-independent manner (12, 16, 17).

FGFR2 targeting siRNA showed a potent growth-inhibitory effect on KATO-III cells. To investigate the dependency of cell growth through activated FGFR2 signaling in the AZD2171-sensitive KATO-III cell line, we evaluated the growth-inhibitory effect of siRNA targeted to FGFR2 in KATO-III cells. Targeted siRNA (5-100 nmol/L) decreased FGFR2 and inhibited cell growth (>80%) in a dose-dependent manner (Fig. 3A). The results show that most of the growth of KATO-III cells is dependent on activated FGFR2 signaling, suggesting that the FGFR signaling dependency may be responsible for the higher growth-inhibitory effect of AZD2171 on KATO-III cells.

AZD2171 inhibited FGFR2 signaling. Next, we examined the effect of AZD2171 on FGFR2 downstream phosphorylation signals (i.e., FRS-2, AKT, and mitogen-activated protein kinase). AZD2171 completely inhibited KGF-induced phosphorylation of FGFR2, FRS-2, AKT, and mitogen-activated protein kinase at 1 μmol/L in KATO-III cells, compared with 10 μmol/L in OKAJIMA cells. These results clearly show that AZD2171 possesses inhibitory activity against FGFR2 in cell-based studies and significantly inhibits the phosphorylation of FGFR2 at 1 μmol/L in sensitive cells.

FGFR2 kinase inhibition of AZD2171. To quantify the inhibitory activity of AZD2171 on FGFR2 kinase under cell-free conditions, we calculated the K_i values for immunoprecipitated FGFR2 derived from KATO-III, OCUM2M, and OKAJIMA cells. The K_i values of AZD2171 for FGFR2 in each of these cell lines were 0.067 ± 0.017, 0.072 ± 0.022, and 0.049 ± 0.041 μmol/L, respectively (Table 1). In contrast, the K_i value of AZD2171 for recombinant VEGFR-2 was 0.0009 μmol/L (data not shown) and was consistent with previous reports (10). At the cellular level, phosphorylation of

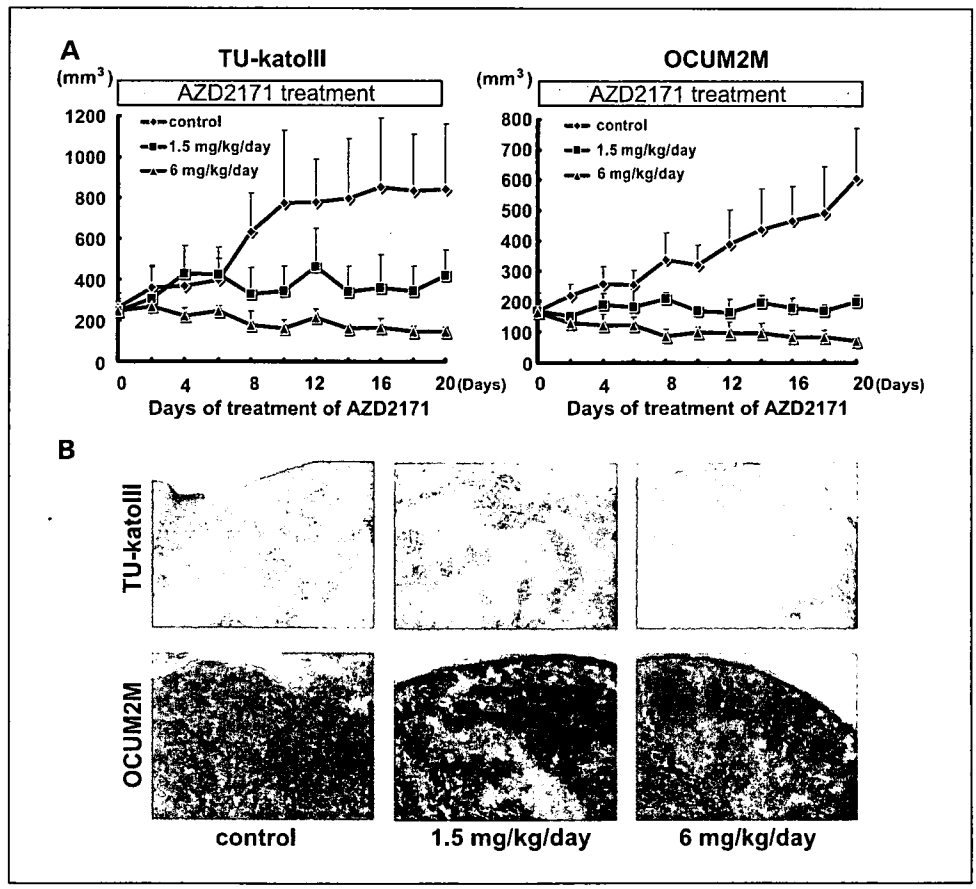

Fig. 4. *A, in vivo* growth-inhibitory effect of AZD2171 in a tumor xenograft model. After s.c. injecting 5×10^6 TU-kato-III or OCUM2M cells into both flanks of the mice, AZD2171 (1.5 or 6.0 mg/kg/d), or vehicle, was administered orally once daily for 3 wks. A marked tumor growth-inhibitory effect was observed at the low dose (1.5 mg/kg/d) of AZD2171 in both the TU-kato-III tumors and OCUM2M tumors, and the high dose (6.0 mg/kg/d) of AZD2171 completely inhibited the growth of both cell lines. *B,* representative H&E staining of tumor tissue from mice treated with AZD2171. Broad dose-dependent necrosis was observed. Original magnification, ×40.

FGFR2 was inhibited at 10-fold lower concentrations of AZD2171 in the sensitive cell lines (Fig. 3B), but there were no marked differences between the kinase-inhibitory effects among the proteins derived from the cell lines in this cell-free assay. This discrepancy is discussed in the Discussion.

In vivo *antitumor activity of AZD2171 against FGFR2-overexpressing gastric cancer.* To elucidate the *in vivo* antitumor activity of AZD2171 in mice bearing gastric cancer tumor xenografts, we used the newly established tumorigenic subline TU-kato-III (derived from KATO-III) and OCCUM2M. We attempted to perform control experiments using OKAJIMA cells *in vivo* as suggested by the reviewer. Unfortunately, however, the cell lines grew slowly in the mice, and we could not precisely evaluate the antitumor activity of AZD2171 in the model. However, the results of preliminarily experiments showed that AZD2171 seemed to be less effective against OKAJIMA cells than against KatoIII and OCUM2M cell *in vivo*. Mice implanted the TU-kato-III and OCUM2M tumors were given a low or high dose of AZD2171 (i.e., 1.5 or 6.0 mg/kg/d), or vehicle, orally for 3 weeks. AZD2171 (1.5 mg/kg/d) significantly inhibited tumor growth in the mice bearing TU-kato-III and OCUM2M tumors, and the higher dose (6.0 mg/kg/d) completely inhibited the growth of both tumor models (Fig. 4A). H&E staining showed broad dose-dependent necrosis of core tumor tissue in mice treated with AZD2171 (Fig. 4B). Thus, AZD2171 showed marked antitumor activity *in vivo* against both human gastric tumor xenografts.

Discussion

Recent studies have shown that FGFRs and their ligands are promising therapeutic target molecules for various malignant diseases, such as prostate cancer (18), breast cancer (5, 19), endometrial carcinoma (20), synovial sarcomas (21), thyroid carcinoma (22, 23), and hematopoietic malignancies (24–27). These findings are based on the biological properties of malignant cells expressing activated FGFR, like FGFR fusion tyrosine kinase, involved in chromosomal translocations, gene amplification of FGFRs, or overexpression of FGFs (5, 18–27). In the case of gastric cancer, the results of immunohistochemical analysis of clinical samples revealed that 20 of 38 cases of advanced undifferentiated type of gastric cancer were FGFR2/K-sam positive, whereas none of the 11 cases with the differentiated or intestinal type of cancer showed positive staining for K-sam (8). The results suggest that FGFR2/K-sam overexpression is associated with the undifferentiated type of stomach cancers. The results of fluorescence *in situ* hybridization analysis of the gastric cancer specimens showed gene amplification of FGFR2/K-sam in 2.9% (28). The clinical implication of FGFR2 overexpression/amplification in gastric cancers remains to be fully clarified, and further investigation is needed.

AZD2171 has the most potent kinase-inhibitory activity against VEGFR-2 (IC_{50} < 1 nmol/L); it also possesses additional activity against VEGFR-1, VEGFR-3, and c-Kit (IC_{50}, 5, ≤3, and 2 nmol/L, respectively; ref. 10). AZD2171 showed antiangiogenic activity and broad antitumor activity consistent with potent inhibition of VEGF-induced angiogenesis. We showed kinase-inhibitory activity of AZD2171 against FGFR2 in the present study. When cancer cells are dependent on FGFR2 signaling, AZD2171 can be expected to give additional therapeutic benefit in addition to its antiangiogenic effects.

A cell-based Western blotting analysis showed that phosphorylation of FGFR2 in KATO-III cells and OCUM2M cells was inhibited by AZD2171 at 10-fold lower dose than in OKAJIMA cells (Fig. 3B). However, there was no significant difference in the K_i values of AZD2171 between the FGFR2 derived from KATO-III, OCUM2M, and OKAJIMA in an *in vitro* kinase assay. This may be attributable to the different conditions between the cell-based and cell-free assays. For example, undefined intrinsic intracellular factors may influence kinase activity: (*a*) differences in baseline intracellular FGFR2 phosphatase activity in each cell line, (*b*) differences in intracellular concentration of ([transporters, such as ATP-binding cassette transporters, may be involved in this phenomenon refs. 29, 30), and (*c*) undefined intrinsic inhibitory factors that bind the compounds directly may also be involved (e.g., Brehmer D, et al. have identified various gefitinib binding proteins by affinity chromatography; ref. 31).

In conclusion, AZD2171, a potent inhibitor of all VEGFRs (VEGFR-1, VEGFR-2, and VEGFR-3), was found to have antitumor effect against gastric cancer xenografts in line with previous findings in colon, lung, prostate, breast, and ovarian tumor xenografts (10). The results of this study suggest that activation of the FGFR2 pathway may be a promising target for gastric cancer therapy. AZD2171 may provide a clinical benefit to gastric cancer patients.

Acknowledgments

We thank Dr. T. Komatsu and M. Takigahira for the animal study and Dr. K. Hirakawa (Osaka City University Graduate School of Medicine, Osaka, Japan) for providing the OCUM2M cell line.

References

1. Vanhoefer U, Rougier P, Wilke H, et al. Final results of a randomized phase III trial of sequential high-dose methotrexate, fluorouracil, and doxorubicin versus etoposide, leucovorin, and fluorouracil versus infusional fluorouracil and cisplatin in advanced gastric cancer: a trial of the European Organization for Research and Treatment of Cancer Gastrointestinal Tract Cancer Cooperative Group. J Clin Oncol 2000;18:2/648–57.
2. Ohtsu A, Shimada Y, Shirao K, et al. Randomized phase III trial of fluorouracil alone versus fluorouracil plus cisplatin versus uracil and tegafur plus mitomycin in patients with unresectable, advanced gastric cancer: The Japan Clinical Oncology Group Study (JCOG9205). J Clin Oncol 2003;21:54–9.
3. Grose R, Dickson C. Fibroblast growth factor signaling in tumorigenesis. Cytokine Growth Factor Rev 2005;16:179–86.
4. Itoh H, Hattori Y, Sakamoto H, et al. Preferential alternative splicing in cancer generates a K-sam messenger RNA with higher transforming activity. Cancer Res 1994;54:3237–41.
5. Moffa AB, Tannheimer SL, Ethier SP. Transforming potential of alternatively spliced variants of fibroblast growth factor receptor 2 in human mammary epithelial cells. Mol Cancer Res 2004;2:643–52.
6. Nakatani H, Sakamoto H, Yoshida T, et al. Isolation of an amplified DNA sequence in stomach cancer. Jpn J Cancer Res 1990;81:707–10.
7. Hattori Y, Odagiri H, Nakatani H, et al. K-sam, an amplified gene in stomach cancer, is a member of the heparin-binding growth factor receptor genes. Proc Natl Acad Sci U S A 1990;87:5983–7.
8. Hattori Y, Itoh H, Uchino S, et al. Immunohistochemical detection of K-sam protein in stomach cancer. Clin Cancer Res 1996;2:1373–81.
9. Ueda T, Sasaki H, Kuwahara Y, et al. Deletion of the carboxyl-terminal exons of K-sam/FGFR2 by short homology-mediated recombination, generating preferential expression of specific messenger RNAs. Cancer Res 1999;59:6080–6.
10. Wedge SR, Kendrew J, Hennequin LF, et al. AZD2171: a highly potent, orally bioavailable, vascular

endothelial growth factor receptor-2 tyrosine kinase inhibitor for the treatment of cancer. Cancer Res 2005;65:4389–400.

11. Arao T, Yanagihara K, Takigahira M, et al. ZD6474 inhibits tumor growth and intraperitoneal dissemination in a highly metastatic orthotopic gastric cancer model. Int J Cancer 2006;118:483–9.
12. Arao T, Fukumoto H, Takeda M, et al. Small in-frame deletion in the epidermal growth factor receptor as a target for ZD6474. Cancer Res 2004;64:9101–4.
13. Taguchi F, Koh Y, Koizumi F, et al. Anticancer effects of ZD6474, a VEGF receptor tyrosine kinase inhibitor, in gefitinib ("Iressa")-sensitive and resistant xenograft models. Cancer Sci 2004;95:984–9.
14. Koizumi F, Kanzawa F, Ueda Y, et al. Synergistic interaction between the EGFR tyrosine kinase inhibitor gefitinib ("Iressa") and the DNA topoisomerase I inhibitor CPT-11 (irinotecan) in human colorectal cancer cells. Int J Cancer 2004;108:464–72.
15. Koizumi F, Shimoyama T, Taguchi F, Saijo N, Nishio K. Establishment of a human non-small cell lung cancer cell line resistant to gefitinib. Int J Cancer 2005; 116:36–44.
16. Sakai K, Arao T, Shimoyama T, et al. Dimerization and the signal transduction pathway of a small in-frame deletion in the epidermal growth factor receptor. FASEB J 2006;20:311–3.17. Duensing A, Heinrich MC, Fletcher CD, Fletcher JA. Biology of gastrointestinal stromal tumors: KIT mutations and beyond. Cancer Invest 2004;22:106–16.
18. Gowardhan B, Douglas DA, Mathers ME, et al. Evaluation of the fibroblast growth factor system as a potential target for therapy in human prostate cancer. Br J Cancer 2005;92:320–7.
19. Zang XP, Nguyen TN, Pento JT. Specific and non-specific KGF inhibition of KGF-induced breast cancer cell motility. Anticancer Res 2002;22:2539–45.
20. Taniguchi F, Harada T, Sakamoto Y, et al. Activation of mitogen-activated protein kinase pathway by keratinocyte growth factor or fibroblast growth factor-10 promotes cell proliferation in human endometrial carcinoma cells. J Clin Endocrinol Metab 2003;88: 773–80.
21. Ishibe T, Nakayama T, Okamoto T, et al. Disruption of fibroblast growth factor signal pathway inhibits the growth of synovial sarcomas: potential application of signal inhibitors to molecular target therapy. Clin Cancer Res 2005;11:2702–12.
22. St Bernard R, Zheng L, Liu W, et al. Fibroblast growth factor receptors as molecular targets in thyroid carcinoma. Endocrinology 2005;146:1145–53.
23. Ezzat S, Huang P, Dackiw A, Asa SL. Clin Dual inhibition of RET and FGFR4 restrains medullary thyroid cancer cell growth. Cancer Res 2005;11:1336–41.
24. Chen J, Lee BH, Williams IR, et al. FGFR3 as a therapeutic target of the small molecule inhibitor PKC412 in hematopoietic malignancies. Oncogene 2005;24: 8259–67.
25. Trudel S, Li ZH, Wei E, et al. CHIR-258, a novel, multitargeted tyrosine kinase inhibitor for the potential treatment of t(4;14) multiple myeloma. Blood 2005; 105:2941–8.
26. Delaval B, Letard S, Lelievre H, et al. Oncogenic tyrosine kinase of malignant hemopathy targets the centrosome. Cancer Res 2005;65:7231–40.
27. Chen J, Deangelo DJ, Kutok JL, et al. PKC412 inhibits the zinc finger 198-fibroblast growth factor receptor 1 fusion tyrosine kinase and is active in treatment of stem cell myeloproliferative disorder. Proc Natl Acad Sci U S A 2004;101:14479–84.
28. Hara T, Ooi A, Kobayashi M, Mai M, Yanagihara K, Nakanishi I. Amplification of c-myc, K-sam, and c-met in gastric cancers: detection by fluorescence *in situ* hybridization. Lab Invest 1998;9:43–53.
29. Yanase K, Tsukahara S, Asada S, Ishikawa E, Imai Y, Sugimoto Y. Gefitinib reverses breast cancer resistance protein-mediated drug resistance. Mol Cancer Ther 2004;3:1119–25.
30. Elkind NB, Szentpetery Z, Apati A, et al. Multidrug transporter ABCG2 prevents tumor cell death induced by the epidermal growth factor receptor inhibitor Iressa (ZD1839, Gefitinib). Cancer Res 2005;65:1770–7.
31. Brehmer D, Greff Z, Godl K, et al. Cellular targets of gefitinib. Cancer Res 2005;65:379–82.

Jpn J Clin Oncol 2007;37(5)358–364
doi:10.1093/jjco/hym033

Serum Total Bilirubin as a Predictive Factor for Severe Neutropenia in Lung Cancer Patients Treated with Cisplatin and Irinotecan

Yutaka Fujiwara, Ikuo Sekine, Yuichiro Ohe, Hideo Kunitoh, Noboru Yamamoto, Hiroshi Nokihara, Yuko Simmyo, Tomoya Fukui, Kazuhiko Yamada and Tomohide Tamura

Division of Internal Medicine and Thoracic Oncology, National Cancer Center Hospital, Tsukiji 5-1-1, Chuo-ku, Tokyo, Japan

Received September 29, 2006; accepted January 5, 2007; published online May 30, 2007

Objective: To clarify the association between pre-treatment total bilirubin (PTB) level and severe toxicity in patients receiving cisplatin and irinotecan.
Methods: We analyzed retrospectively the relationships of grade 4 neutropenia or grade 3–4 diarrhea and clinical variables including PTB and pre-treatment neutrophil counts (PNC) using a logistic regression model.
Results: One hundred and twenty-seven patients (93 men, 34 women; median age: 61 years; range: 24–74 years) received cisplatin (60 or 80 mg/m^2) on day 1 and irinotecan (60 mg/m^2) on days 1 and 8 every 3 weeks or on days 1, 8 and 15 every 4 weeks. Grade 4 neutropenia occurred in 29 patients (23%) and grade 3–4 diarrhea occurred in 13 patients (10%). Grade 4 neutropenia was associated with a higher PTB level (odds ratio: 4.9; 95% confidence interval: 1.4–17.7), a higher cisplatin dose (2.8, 1.0–7.8) and a lower PNC (1.5, 1.0–2.3). Grade 3–4 diarrhea was associated with liver metastasis (11.2, 2.2–57.4), a higher cisplatin dose (5.0, 1.2–21.3) and a lower PNC (2.0, 1.1–3.6).
Conclusions: PTB level was associated with the severity of neutropenia caused by cisplatin and irinotecan.

Key words: irinotecan – toxicity – lung cancer

INTRODUCTION

Although irinotecan is an active agent against several solid tumors, it sometimes exhibits serious adverse effects, the most common being bone marrow toxicity, in particular leucopenia and neutropenia, and ileocolitis, which leads to diarrhea (1–4). The severity of these toxicities varies greatly between individuals, and thus identifying pre-treatment factors that predict an increased risk for severe toxicities is a critical issue in the treatment of cancer patients undergoing chemotherapy.

Irinotecan needs to be activated by systemic carboxylesterases to SN-38 to exert its anti-tumor activity, which is mediated by the inhibition of topoisomerase I (5). Glucuronidation of SN-38 (SN-38G) by UDP-glucuronosyltransferase (UGT) 1A1 during biliary excretion is the primary route of detoxification and elimination. A higher ratio of plasma SN-38 to SN38-G has been correlated with severe diarrhea, suggesting that the efficiency of SN-38 glucuronidation is an important determinant of toxicity (6–8).

Genetic polymorphisms of the UGT 1A1 gene, such as the number of TA repeats in the TATA box that are associated with reduced transcriptional efficiency and functional activity, have been reported previously (7). Some studies have demonstrated an association between UGT1A1 polymorphisms and the risk for severe toxicity from irinotecan (6, 8–11).

The UGT1A1 enzyme is also responsible for hepatic bilirubin glucuronidation. Serum bilirubin levels, therefore, may reflect UGT1A1 activity and may also be associated with irinotecan activity and toxicity. The pre-treatment serum total bilirubin (PTB) level has been shown to be related to

For reprints and all correspondence: Division of Internal Medicine and Thoracic Oncology, National Cancer Center Hospital, Tsukiji 5-1-1, Chuo-ku, Tokyo 104-0045, Japan. E-mail: isekine@ncc.go.jp

© 2007 Foundation for Promotion of Cancer Research

severe neutropenia in patients receiving 350 mg/m^2 of irinotecan (8). We extended this observation in patients receiving cisplatin and irinotecan to clarify the association between PTB and severe toxicity, including neutropenia and diarrhea, in these patients.

PATIENTS AND METHODS

Treatment Schedule

The subjects consisted of consecutive lung cancer patients who had received cisplatin and irinotecan therapy at the National Cancer Centre Hospital between February 1999 and May 2004. Irinotecan, diluted in 500 ml of normal saline, was given intravenously over 90 min at a dose of 60 mg/m^2 on days 1 and 8 or on days 1, 8 and 15. Cisplatin was given intravenously over 60 min after the irinotecan infusion at a dose of 60 or 80 mg/m^2 on day 1 with at least 2500 ml of hydration. The first phase I trial of irinotecan and cisplatin showed that 80 mg/m^2 of cisplatin on day 1 and 60 mg/m^2 of irinotecan on days 1, 8, and 15 were the recommended dose for phase II trials (12), and this dose schedule was used for subsequent phase II and phase III trials of non-small cell lung cancer (NSCLC) (13,4,14). The second phase I trial of this combination showed that 60 mg/m^2 of cisplatin on day 1 and 80 mg/m^2 of irinotecan on days 1, 8, and 15 were the recommended dose (15). A phase II trial for small cell lung cancer, however, showed that this dose schedule was too toxic, and thereafter the dose of irinotecan was reduced from 80 to 60 mg/m^2 (16). From the above, we used 80 mg/m^2 of cisplatin and 60 mg/m^2 of irinotecan for patients with NSCLC, and 60 mg/m^2 of cisplatin and 60 mg/m^2 of irinotecan for the other patients. Administration of irinotecan was omitted if any of the following toxicities were noted on days 8 and 15: a white blood cell count $<2.0 \times 10^9$/l, a platelet count $<75 \times 10^9$/l, or grade 1–3 diarrhea. Each course was repeated every 3 or 4 weeks until the occurrence of unacceptable toxicity, disease progression, patient's refusal to continue treatment, or the investigator's medical decision to stop treatment. To control for cisplatin-induced emesis, a 5-HT3 receptor antagonist and dexamethasone were given prior to cisplatin administration.

Study Design

We retrospectively reviewed the patients' clinical records, including patient characteristics (age, sex, Eastern Cooperative Oncology Group performance status, histology of primary disease, clinical stage, prior treatment, evidence of liver metastasis), the dose and schedule of chemotherapy, and pre-treatment complete blood counts and serum chemistry profiles. We defined 'severe toxicity' as grade 4 neutropenia or grade 3–4 diarrhea during the first cycle of chemotherapy, in accordance with the NCI-CTC Version 2.0 criteria. All patients were treated as in-patients, and complete blood counts and serum chemistry profiles were assessed at least once a week. PTB was defined as the serum total bilirubin level at fasting just prior to the administration of cisplatin and irinotecan.

Table 1. Patient characteristics

		No. of patients
Sex	Male/female	93/34
Age	Median (range)	61 (24–74)
Performance status	0/1/2	34/91/2
Histology	Non-small cell lung cancer	57
	Small cell lung cancer	63
	Others	7
Liver metastasis	Yes/no	18/109
Prior chemotherapy	Yes/no	17/110
PTB (mg/m^2)	Median (range)	0.6 (0.2–2.4)
PNC ($\times 10^9$/l)	Median (range)	4.1 (1.8–8.5)
Chemotherapy	CDDP (60) day 1 + CPT-11 (60) days 1.8 q3w	32
Regimens (mg/dl)	CDDP (60) day 1 + CPT-11 (60) days 1.8.15 q4w	39
	CDDP (80) day 1 + CPT-11 (60) days 1.8 q3w	24
	CDDP(80) day1 + CPT-11 (60) days 1.8.15 q4w	32

PTB, pre-treatment total bilirubin; PNC, pre-treatment neutrophil count.

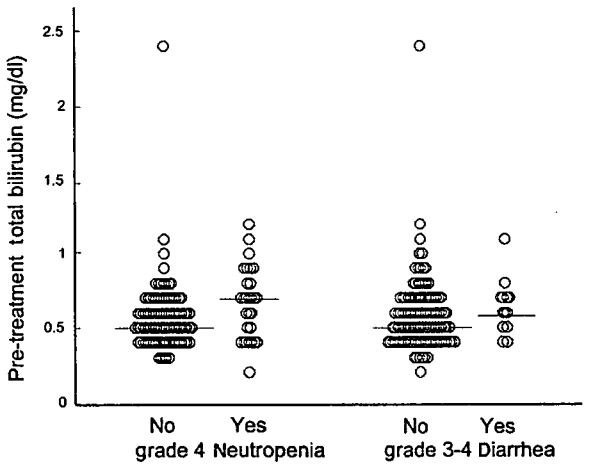

Figure 1. Association of PTB in patients who developed severe toxicity and in those who did not. The median PTB in patients who developed grade 4 neutropenia and those who did not was 0.7 (range, 0.2–1.2) mg/dl and 0.5 (range, 0.3–2.4) mg/dl, respectively ($P = 0.03$, Mann–Whitney U test). The median PTB in patients who developed grade 3–4 diarrhea and those who did not was 0.6 and 0.5 mg/dl, respectively ($P = 0.22$). The bars represent the median values.

Table 2. Univariate analysis of association between grade 4 neutropenia and pre-treatment clinical variables

	Neutropenia grade		Odds ratio (95% CI)
	Grade <4 ($n = 98$)	Grade 4 ($n = 29$)	
Sex			
Male	70	23	1
Female	28	6	0.65 (0.24–1.77)
Age			
Median (range)	61 (24–74)	65 (38–73)	1.04 (0.99–1.09)
Performance status			
0	29	5	1
1, 2	69	24	2.02 (0.70–5.80)
Liver metastasis			
No	82	27	1
Yes	16	2	0.38 (0.08–1.76)
Prior chemotherapy			
No	84	26	1
Yes	14	3	0.69 (0.19–2.60)
Treatment schedule			
Every 3 weeks	41	15	1
Every 4 weeks	57	14	0.67 (0.29–1.54)
Cisplatin dose (mg/m^2)			
60	56	15	1
80	42	14	1.24 (0.54–2.86)
AST (IU/l)			
Median (range)	22 (11–161)	22 (11–56)	0.98 (0.95–1.01)
ALT (IU/l)			
Median (range)	18 (6–266)	20 (5–67)	0.99 (0.97–1.02)
PNC ($\times 10^9$/l)			
Median (range)	4.4(2.0–8.5)	3.9 (1.8–8.3)	0.84 (0.61–1.14)
PTB (mg/dl)			
Median (range)	0.5 (0.3–2.4)	0.7 (0.2–1.2)	3.74 (0.70–19.9)
≤0.7	87	20	1
>0.7	11	9	3.56 (1.30–9.73)

AST, aspartate aminotransferase; ALT, alanine aminotransferase; PNC, pre-treatment neutrophil count; PTB, pre-treatment total bilirubin.

Statistical Methods

The Mann–Whitney U test was used to compare the PTB levels of patients who developed severe toxicity and those who did not. Possible explanatory factors were compared using a logistic regression model. A PTB threshold of ≤0.7 mg/dl was selected to categorize this variable because a total bilirubin level higher than 0.7 mg/dl has been correlated with a mutated UGT1A1 genotype and the occurrence of grade 4 neutropenia (8). Furthermore, sex, performance status, liver metastasis, prior chemotherapy, treatment schedule and cisplatin dose were defined as categorized variables, and age, AST, ALT and pre-treatment neutrophil count (PNC) were examined as continuous variables. Variables that seemed to be associated with severe toxicity ($P < 0.1$) were considered for inclusion in a multivariate analysis using a backward stepwise regression model. We performed these analyses using the SPSS statistical package (SPSS version 11.0 for Windows; SPSS Inc., Chicago, IL, USA).

RESULTS

A total of 127 consecutive patients with thoracic malignancy received cisplatin and irinotecan therapy. The patient characteristics are listed in Table 1. In all, two patients (1.5%) had

Table 3. Backward stepwise regression analysis of association between severe toxicity and pre-treatment clinical variables

Variable	Co-efficient	*P*	Odds ratio (95% CI)
Grade 4 neutropenia			
Cisplatin dose	1.04	0.04	2.84 (1.03–7.81)
PNC	0.42	0.04	1.53 (1.02–2.27)
PTB	1.59	0.02	4.93 (1.37–17.7)
Grade 3–4 diarrhea			
Liver metastasis	2.41	0.004	11.2 (2.18–57.4)
Cisplatin dose	1.61	0.03	5.00 (1.18–21.3)
PNC	0.67	0.03	1.96 (1.07–3.60)

Adjusted for age and PS.
PNC, pre-treatment neutrophil count; PTB, pre-treatment total bilirubin.

stage IIA disease, seven patients (5.5%) had stage IIIA disease, 26 patients (20%) had stage IIIB disease and 85 patients (67%) had stage IV disease. The median PTB level was 0.6 (range, 0.2–2.4) mg/dl and the median PNC was 4.1 (range 1.8–8.5) $\times 10^9$/l. A total of 93 patients (73%) received the planned doses without skipping the irinotecan administrations on day 8 or 15. Among the remaining 34 patients, the irinotecan on day 8 or 15 was omitted in 27 of 164 (16.5%) planned doses in patients with PTB level $\leq$0.7 mg/dl, while in 11 of 34 (32.4%) planned doses in patients with PTB level >0.7 mg/dl ($P = 0.053$). Thus, the actual irinotecan dose delivered was lower with marginal significance in patients with PTB level >0.7 mg/dl. Grade 4 neutropenia occurred in 29 (23%) patients and grade 3–4 diarrhea occurred in 13 (10%) patients.

The median PTB level was higher in patients who developed grade 4 neutropenia than in those who did not (0.7 and 0.5 mg/dl, respectively; $P = 0.03$) (Fig. 1), but PTB was not correlated with the presence or absence of grade 3–4 diarrhea ($P = 0.22$).

In a univariate analysis, grade 4 neutropenia was associated with only the PTB level ($\leq$0.7 versus >0.7 mg/dl; $P = 0.01$, Table 2). When PTB level was analyzed as a continuous variable, the association was not significant (OR: 3.74; 95% CI: 0.70–19.9; $P = 0.12$). In a multivariate analysis, grade 4 neutropenia was associated with the PTB level ($\leq$0.7 versus >0.7 mg/dl; $P = 0.02$), the cisplatin dose ($P = 0.04$), and PNC ($P = 0.04$, Table 3). In a univariate analysis, grade 3–4 diarrhea was associated with only liver metastasis ($P = 0.01$, Table 4). We analyzed serum levels of PTB and pre-treatment AST and ALT between patients with ($n = 18$) or without ($n = 109$) liver metastasis. The median (range) PTB was 0.6 (0.4–2.4) mg/dl in patients with liver metastasis and 0.6 (0.2–1.2) mg/dl in patients without liver metastasis ($p = 0.19$). In contrast, the median (range) levels of pre-treatment AST and ALT were 30 (16–114) IU/l and 30 (11–84) IU/l, respectively, in patients with liver metastasis and 21 (11–161) IU/l and 17 (5–266) IU/l, respectively, in patients without liver metastasis ($P = 0.0054$). In a multivariate analysis, grade 3–4 diarrhea was associated with liver metastasis ($P = 0.004$), the cisplatin dose ($P = 0.03$) and PNC ($P = 0.03$, Table 4).

DISCUSSION

This study showed that the PTB level was significantly associated with severity of neutropenia in patients treated with cisplatin and weekly irinotecan. Although irinotecan-induced toxicity can be reduced by skipping irinotecan on day 8, 15, or both, this dose modification is not enough to eliminate severe toxicity completely. In this study irinotecan was more frequently omitted on days 8 and 15 in patients with PTB level >0.7 mg/dl, and therefore, the association between PTB and irinotecan-induced toxicity may be underestimated. Thus, the PTB level, a simple routine measure in clinical practice, can be a useful predictive marker for irinotecan-induced toxicity.

The most compelling evidence for a genetic marker of toxicity caused by irinotecan therapy is seen with the *UGT* gene. In some retrospective pharmacogenetic studies, patients with at least one *UGT*1A1*28 allele encountered severe irinotecan-induced toxicity, compared with those with the wild-type genotype who were homozygous for the 6 TA repeat allele (6,9,10). In a prospective study, the *UGT*1A1 genotype was strongly associated with severe neutropenia in patients treated with irinotecan (8). More than 30 polymorphic variations have been reported to date for the *UGT*1A1 gene (17). Novel polymorphisms (*1, *6, *28,*60 and so on) in *UGT*1A1 and the functional characterization of known variants are helpful in elucidating the role of *UGT*1A1 genetic variation in irinotecan toxicity (18). The FDA has approved a *UGT*1A1 molecular assay test to detect polymorphisms in the *UGT*1A1 gene in clinical practice, so that patients with particular *UGT*1A1 gene variations that raise the risk of certain adverse effects can receive safer doses of irinotecan. This assay is intended to aid physicians to make decisions for individualized patient. Nevertheless, other important factors that affect dosing should also be considered, because severe toxicity sometimes occurs even in patients without particular *UGT*1A1 gene variations that place them at risk.

The *UGT*1A1 enzyme is responsible for hepatic bilirubin glucuronidation. A polymorphism in the *UGT*1A1 promoter has been linked with reduced *UGT*1A1 expression and is consequently associated with familiar hyperbilirubinemia. Accordingly, bilirubin levels may be associated with *UGT*1A1 function. The PTB level may reflect the total function of some polymorphisms in the *UGT*1A1 region and may be used as a simple and available surrogate marker for *UGT*1A1 function.

Recent studies have revealed that two major hepatic UGT, *UGT*1A1 and *UGT*1A9, and extra-hepatic *UGT*1A7 are involved in SN-38 glucuronidation (SN-38G) (7,19). The

Table 4. Univariate analysis of association between grade 3–4 diarrhea and pre-treatment clinical variables

	Diarrhea grade		Odds ratio (95% CI)
	Grade 0–2 ($n = 114$)	Grade 3–4 ($n = 13$)	
Sex			
Male	84	9	1
Female	30	4	1.24 (0.36–4.34)
Age			
Median (range)	65 (24–74)	65 (53–73)	1.07 (0.99–1.16)
Performance status			
0	29	5	1
1, 2	85	8	0.55 (0.17–1.80)
Liver metastasis			
No	101	8	1
Yes	13	5	4.86 (1.38–17.1)
Prior chemotherapy			
No	99	11	1
Yes	15	2	1.20 (0.20–7.04)
Treatment schedule			
Every 3 weeks	50	6	1
Every 4 weeks	64	7	0.91 (0.29–2.88)
Cisplatin dose (mg/m^2)			
60	66	5	1
80	48	8	2.20 (0.68–7.14)
AST (IU/l)			
Median (range)	21 (11–161)	23 (15–65)	1.00 (0.98–1.03)
ALT (IU/l)			
Median (range)	17 (5–266)	21 (14–84)	1.01 (0.99–1.02)
PNC ($\times 10^9$/l)			
Median (range)	4.2 (1.8–8.5)	3.5 (2.2–5.2)	0.77 (0.49–1.20)
PTB (mg/dl)			
Median (range)	0.55 (0.2–2.4)	0.6 (0.4–1.1)	1.95 (0.29–13.2)
≤ 0.7	96	11	1
>0.7	18	2	0.97 (0.20–4.75)

AST, aspartate aminotransferase; ALT, alanine aminotransferase; PNC, pre-treatment neutrophil count; PTB, pre-treatment total bilirubin.

efficacy of irinotecan is possibly affected by the activity of these genes. Thus, the product of some genetic polymorphisms in several genes may be a better pharmacogenetic marker for selecting patients who may not respond favorably to irinotecan-containing chemotherapy.

Cisplatin and irinotecan therapy is a standard regimen for both advanced non-small cell and small cell lung cancer (4). A randomized trial of irinotecan with or without cisplatin in patients with non-small cell lung cancer showed that grade 4 neutropenia was observed more frequently in the cisplatin–irinotecan arm (37%) than in the irinotecan-alone arm (8%), whereas grade 3 and 4 diarrhea was observed at the same frequency in both arms. In the present study, a higher cisplatin dose was associated with both grade 4 neutropenia and grade 3 and 4 diarrhea. The addition of cisplatin to another anti-cancer agent aggravated diarrhea in phase III studies (20), although diarrhea was moderate in cisplatin monotherapy observed in clinical trials (21). Thus, a higher dose of cisplatin seems to be associated with diarrhea, but the mechanism for this association remains unclear.

In this study PTB level was associated with the severity of neutropenia, but not with severity of diarrhea. When SN-38G is excreted in the bile and intestines, the bacteria-derived enzyme beta-glucuronidase converts SN-38G back

into SN-38 (22,23). Presence of SN-38 in the stool is associated with the occurrence of severe diarrhea as a result of the direct enteric injury caused by SN-38 (24). This phenomenon probably occurs because UGT1A1 is not involved in this step.

Liver metastasis was associated with the development of grade 3–4 diarrhea in both univariate and multivariate analyses in this study. This may be explained by small, but statistically significant differences in the pre-treatment transaminase levels between patients with or without liver metastasis. However, in contradiction to this explanation are that: (1) neither the pre-treatment AST nor ALT level was associated with grade 3–4 diarrhea in this study, and (2) in dose-finding studies of irinotecan monotherapy in patients with liver dysfunction, patients were categorized into subgroups by the PTB and serum AST and ALT levels, criteria of which were three times or five times the upper limit of normal (25,26). Thus, the small difference in the AST and ALT levels in this study is unlikely to be significant from the medical point of view.

The PNC in patients who developed grade 3–4 diarrhea was slightly lower than that in the other patients and the PNC was associated with grade 3–4 diarrhea in the multivariate analysis. Neutrophils play an important role in maintaining the mucosal barrier of the intestine and inflammatory responses against mucosal damage (27). Thus, reduced number, dysfunction, or both, of neutrophils may lead to impairment of the mucosal integrity, rendering these patients prone to develop diarrhea. In addition, the decreased number of neutrophils in the blood is closely related to malnutrition associated with cancer (28), which may in turn be associated with enhanced toxicity during chemotherapy with irinotecan and cisplatin.

In conclusion, the PTB level was significantly associated with severity of neutropenia in patients treated with cisplatin and weekly irinotecan. This will provide a simple and useful marker required for individualized therapy to reduce the risk of harmful chemotherapy.

Acknowledgments

We thank Mika Nagai for her assistance with the preparation of the manuscript.

Conflict of interest statement

None declared.

References

1. Negoro S, Fukuoka M, Masuda N, Takada M, Kusunoki Y, Matsui K, et al. Phase I study of weekly intravenous infusions of CPT-11, a new derivative of camptothecin, in the treatment of advanced non-small-cell lung cancer. *J Natl Cancer Inst* 1991;83:1164–8.
2. Rothenberg ML, Kuhn JG, Burris HA, Nelson J, 3rd, Eckardt JR, Tristan-Morales M, et al. Phase I and pharmacokinetic trial of weekly CPT-11. *J Clin Oncol* 1993;11:2194–204.
3. Saltz LB, Cox JV, Blanke C, Rosen LS, Fehrenbacher L, Moore MJ, et al. Irinotecan plus fluorouracil and leucovorin for metastatic colorectal cancer. Irinotecan Study Group. *N Engl J Med* 2000;343:905–14.
4. Negoro S, Masuda N, Takada Y, Sugiura T, Kudoh S, Katakami N, et al. Randomised phase III trial of irinotecan combined with cisplatin for advanced non-small-cell lung cancer. *Br J Cancer* 2003;88:335–41.
5. Iyer L, King CD, Whitington PF, Green MD, Roy SK, Tephly TR, et al. Genetic predisposition to the metabolism of irinotecan (CPT-11). Roleof uridine diphosphate glucuronosyltransferase isoform 1A1 in the glucuronidation of its active metabolite (SN-38) in human liver microsomes. *J Clin Invest* 1998;101:847–54.
6. Ando Y, Saka H, Ando M, Sawa T, Muro K, Ueoka H, et al. Polymorphisms of UDP-glucuronosyltransferase gene and irinotecan toxicity: a pharmacogenetic analysis. *Cancer Res* 2000;60:6921–6.
7. Gagne JF, Montminy V, Belanger P, Journault K, Gaucher G, Guillemette C. Common human UGT1A polymorphisms and the altered metabolism of irinotecan active metabolite 7-ethyl-10-hydroxycamptothecin (SN-38). *Mol Pharmacol* 2002;62:608–17.
8. Innocenti F, Undevia SD, Iyer L, Chen PX, Das S, Kocherginsky M, et al. Genetic variants in the UDP-glucuronosyltransferase 1A1 gene predict the risk of severe neutropenia of irinotecan. *J Clin Oncol* 2004;22:1382–8.
9. Iyer L, Das S, Janisch L, Wen M, Ramirez J, Karrison T, et al. *UGT*1A1*28 polymorphism as a determinant of irinotecan disposition and toxicity. *Pharmacogenomics J* 2002;2:43–7.
10. Marcuello E, Altes A, Menoyo A, Del Rio E, Gomez-Pardo M, Baiget M. *UGT*1A1 gene variations and irinotecan treatment in patients with metastatic colorectal cancer. *Br J Cancer* 2004;91:678–82.
11. Rouits E, Boisdron-Celle M, Dumont A, Guerin O, Morel A, Gamelin E. Relevance of different *UGT*1A1 polymorphisms in irinotecan-induced toxicity: a molecular and clinical study of 75 patients. *Clin Cancer Res* 2004;10:5151–9.
12. Masuda N, Fukuoka M, Takada M, Kusunoki Y, Negoro S, Matsui K, et al. CPT-11 in combination with cisplatin for advanced non-small-cell lung cancer. *J Clin Oncol* 1992;10:1775–80.
13. Masuda N, Fukuoka M, Fujita A, Kurita Y, Tsuchiya S, Nagao K, et al. A phase II trial of combination of CPT-11 and cisplatin for advanced non-small-cell lung cancer. CPT-11 Lung Cancer Study Group. *Br J Cancer* 1998;78:251–6.
14. Niho S, Nagao K, Nishiwaki Y, Yokoyama A, Saijo N, Ohashi Y, et al. Randomized multicenter phase III trial of irinotecan and cisplatin versus cisplatin and vindesine in patients with advanced non-small-cell lung cancer. *Proc Am Soc Clin Oncol* 1999;18:p492a.
15. Masuda N, Fukuoka M, Kudoh S, Kusunoki Y, Matsui K, Takifuji N, et al. Phase I and pharmacologic study of irinotecan in combination with cisplatin for advanced lung cancer. *Br J Cancer* 1993;68:777–82.
16. Kudoh S, Fujiwara Y, Takada Y, Yamamoto H, Kinoshita A, Ariyoshi Y, et al. Phase II study of irinotecan combined with cisplatin in patients with previously untreated small-cell lung cancer. West Japan Lung Cancer Group. *J Clin Oncol* 1998;16:1068–74.
17. Burchell B, Hume R. Molecular genetic basis of Gilbert's syndrome. *J Gastroenterol Hepatol* 1999;14:960–6.
18. Sai K, Saeki M, Saito Y, Ozawa S, Katori N, Jinno H, et al. *UGT*1A1 haplotypes associated with reduced glucuronidation and increased serum bilirubin in irinotecan-administered Japanese patients with cancer. *Clin Pharmacol Ther* 2004;75:501–15.
19. Jinno H, Tanaka-Kagawa T, Hanioka N, Saeki M, Ishida S, Nishimura T, et al. Glucuronidation of 7-ethyl-10-hydroxycamptothecin (SN-38), an active metabolite of irinotecan (CPT-11), by human *UGT*1A1 variants, G71R, P229Q, and Y486D. *Drug Metab Dispos* 2003;31:108–13.
20. Le Chevalier T, Brisgand D, Douillard JY, Pujol JL, Alberola V, Monnier A, et al. Randomized study of vinorelbine and cisplatin versus vindesine and cisplatin versus vinorelbine alone in advanced non-small-cell lung cancer: results of a European multicenter trial including 612 patients. *J Clin Oncol* 1994;12:360–7.
21. Arnold RJ, Gabrail N, Raut M, Kim R, Sung JC, Zhou Y. Clinical implications of chemotherapy-induced diarrhea in patients with cancer. *J Support Oncol* 2005;3:227–32.
22. Mathijssen RH, Loos WJ, Verweij J, Sparreboom A. Pharmacology of topoisomerase I inhibitors irinotecan (CPT-11) and topotecan. *Curr Cancer Drug Targets* 2002;2:103–23.

23. Yokoi T, Narita M, Nagai E, Hagiwara H, Aburada M, Kamataki T. Inhibition of UDP-glucuronosyltransferase by aglycons of natural glucuronides in kampo medicines using SN-38 as a substrate. *Jpn J Cancer Res* 1995;86:985–9.
24. Araki E, Ishikawa M, Iigo M, Koide T, Itabashi M, Hoshi A. Relationship between development of diarrhea and the concentration of SN-38, an active metabolite of CPT-11, in the intestine and the blood plasma of athymic mice following intraperitoneal administration of CPT-11. *Jpn J Cancer Res* 1993;84:697–702.
25. Venook AP, Enders Klein C, Fleming G, Hollis D, Leichman CG, et al. A phase I and pharmacokinetic study of irinotecan in patients with hepatic or renal dysfunction or with prior pelvic radiation: CALGB 9863. *Ann Oncol* 2003;14:1783–90.
26. Schaaf LJ, Hammond LA, Tipping SJ, Goldberg RM, Goel R, Kuhn JG, et al. Phase I and pharmacokinetic study of intravenous irinotecan in refractory solid tumor patients with hepatic dysfunction. *Clin Cancer Res* 2006;12:3782–91.
27. Sartor RB. Mucosal immunology and mechanisms of gastrointestinal inflammation. In: Feldman M, Friedman LS, Sleisenger MH editors. Gastrointestinal and Liver Disease, 7th edn. Philadelphia, PA: Saunders 2002; 21–51.
28. Balducci L, Little DD, Glover NG, Hardy CS, Steinberg MH. Granulocyte reserve in cancer and malnutrition. *Ann Intern Med* 1983;98:610–1.

Bodyweight change during the first 5 days of chemotherapy as an indicator of cisplatin renal toxicity

Ikuo Sekine,[1] Kazuhiko Yamada, Hiroshi Nokihara, Noboru Yamamoto, Hideo Kunitoh, Yuichiro Ohe and Tomohide Tamura

Division of Internal Medicine and Thoracic Oncology, National Cancer Center Hospital, Tsukiji 5-1-1, Chuo-ku, Tokyo 104-0045, Japan

(Received Feburary 22, 2007/Revised April 25, 2007/Accepted April 27, 2007/Online publication June 26, 2007)

To determine whether bodyweight (BW) loss, daily urine volume (UV) or furosemide use are associated with cisplatin nephrotoxicity, performance status, serum chemistries before treatment, average daily UV, maximum BW loss and use of furosemide on days 1–5 of chemotherapy were evaluated retrospectively in chemotherapy-naive patients with thoracic malignancies who had received 80 mg/m² cisplatin. Associations between these parameters and the worst serum creatinine levels (group 1, grade 0–1; and group 2, grade 2–3) during the first cycle were evaluated. Of the 417 patients (327 men and 90 women; median age, 59 years), 390 were categorized into group 1 and 27 were categorized into group 2. More women and older patients were observed in group 2 than in group 1 (11.1 *vs* 5.2%, $P = 0.044$, and 65 *vs* 59 years, $P = 0.041$, respectively). The median average daily UV was 3902 mL in group 1 and 3600 mL in group 2 ($P = 0.021$). A maximum BW loss ≥2.1 kg was noted in 4.4% of patients in group 1 and 18.5% of patients in group 2 ($P = 0.006$). Furosemide was used in 206 (49.4%) patients. The median total dose of furosemide in groups 1 and 2 were 0 mg and 26 mg, respectively ($P = 0.024$). A multivariate analysis showed that a maximum BW loss ≥2.1 kg and the total furosemide dose were significantly associated with group category. In conclusion, BW loss and total furosemide dose were associated with cisplatin nephrotoxicity. (*Cancer Sci* 2007; 98: 1408–1412)

Cisplatin alone or in combination with other chemotherapeutic agents has been the most frequently used chemotherapy regimen against a variety of solid tumors for 30 years because of its significant therapeutic effects.[1] In spite of intensive efforts to devise platinum analogs and the successful development of carboplatin, cisplatin remains a key agent in the treatment of germ cell tumors, head and neck cancer and bladder cancer, as shown in several randomized controlled trials comparing the two platinum agents.[2] In addition, cisplatin has a significant role in the treatment of lung and ovarian cancers, although carboplatin is becoming increasingly used against these cancers as an alternative chemotherapeutic agent.[3,4]

Cisplatin nephrotoxicity has been a major dose-limiting toxicity for this drug in most drug administration schedules.[5] Although the exact mechanism is unclear, high concentrations of platinum and widespread necrosis were observed in the proximal tubules of the kidney. This tubular impairment secondarily leads to a reduction in renal blood flow and glomerular filtration rate, potentiating primary tubular damage. This vicious circle causes a delayed deterioration in renal function, as an increase in the serum creatinine level typically appears 6–7 days after cisplatin administration in humans.[5,6] The standard prophylaxis for cisplatin nephrotoxicity is a normal saline infusion of 1–4 L with osmotic diuresis on the day of cisplatin administration.[5] Although this vigorous hydration diminishes life-threatening renal toxicity, 7–40% of patients still develop a mild to moderate increase in their serum creatinine levels, which influences subsequent cisplatin therapy.[7,8] For the prevention of cisplatin nephrotoxicity, the maintenance of good renal hemodynamics may be necessary for a week or longer after cisplatin administration, although indicators of hydration management on day 2 of chemotherapy and thereafter have not been reported. The purpose of this retrospective study was to evaluate bodyweight (BW) changes, daily urine volumes (UV) and use of furosemide on days 1–5 of chemotherapy as well as pretreatment patient characteristics in the hope of finding an association between these factors and nephrotoxicity during the first cycle of cisplatin-based chemotherapy.

Patients and Methods

Patient selection. Patients were selected retrospectively for the present study according to the following criteria: (1) a histological or cytological diagnosis of thoracic malignancy; (2) no prior chemotherapy; (3) a chemotherapy treatment regimen that included 80 mg/m² of cisplatin; and (4) treatment as an in-patient at the National Cancer Center Hospital. Patients were excluded if: (1) their pretreatment serum creatinine level was abnormal; or (2) no record of BW or daily UV on days 1–5 of chemotherapy was available.

Treatment. Cisplatin at a dose of 80 mg/m² was administered intravenously over 60 min on day 1 in combination with other chemotherapeutic agents. Hydration just before cisplatin administration consisted of 500 mL normal saline, 500 mL 5% glucose and 10 mL KCl over 4 h. Hydration just after cisplatin infusion consisted of 500 mL normal saline with 40 g mannitol over 2 h, followed by 500 mL normal saline, 1000 mL 5% glucose and 15 mL KCl over 6 h. On days 2–5, 1000 mL normal saline, 1000 mL 5% glucose and 20 mL KCl were administered over 8 h. Antiemetic prophylaxis consisted of a $5HT_3$ antagonist and 16 mg dexamethasone on day 1 followed by 8 mg dexamethasone on days 2 and 3, 4 mg on day 4 and 2 mg on day 5. Furosemide was given orally or intravenously if fluid retention was suspected based on an increased BW or a decreased UV. These treatments were repeated every 3–4 weeks.

Data collection and statistical analyses. The patients' baseline characteristics, including age, sex and performance status as well as serum albumin, Na, K, Ca and fasting blood sugar levels were analyzed. The modified Ca level was calculated using the following formula:

$$\text{modified Ca (mg/dL)} = \text{serum Ca (mg/dL)} + 4 - \text{serum albumin (g/dL)}.$$

The daily UV and BW at 0800 hours (before breakfast) and at 1600 hours (before dinner) were measured once a day on days

[1]To whom correspondence should be addressed. E-mail: isekine@ncc.go.jp

doi: 10.1111/j.1349-7006.2007.00532.x
© 2007 Japanese Cancer Association

Table 1. Patient demographics and pretreatment blood chemistry tests in groups categorized according to worst creatinine grade

		Group 1 (n = 390)		Group 2 (n = 27)		P-value
		n	%	n	%	
Sex	Male	310	94.8	17	5.2	0.044
	Female	80	88.9	10	11.1	
Age (years)	Median	59	(Range 18–77)	65	(Range 38–74)	0.041
Performance status	0	169	92.3	14	7.7	0.82
	1	218	94.3	13	5.6	
	2–3	3	100	0	0	
Serum albumin	≥3.7 g/dL	319	94.1	20	5.9	0.32
	≤3.6 g/dL	71	91.0	7	9.0	
Serum Na	≥138 mEq/L	341	93.2	25	6.8	0.43
	≤137 mEq/L	49	96.1	2	3.9	
Serum K	≤4.9 mEq/L	373	93.7	25	6.3	0.46
	≥5.0 mEq/L	17	89.5	2	10.5	
Modified Ca†	≤10.4 mg/dL	376	93.3	27	6.7	0.31
	≥10.5 mg/dL	14	100	0	0	
Fasting blood sugar	≤125 mg/dL	322	92.8	25	7.2	0.36
	≥126 mg/dL	54	96.4	2	3.6	
	Not done	14	100	0	0	

†Calculated using the equation: modified Ca (mg/dL) = serum Ca (mg/dL) + 4 − serum albumin (g/dL). Groups 1 and 2 were patients with worst creatinine grades of 0–1 and 2–3, respectively.

1–5 of the chemotherapy regimens. The BW at 0800 hours on day 1 was used as the baseline BW. During the chemotherapy course, blood chemistry was analyzed at least once a week. Data on furosemide use and the BW gain just before furosemide use during the first course of chemotherapy were obtained from medical charts.

The worst serum creatinine level during the first course of chemotherapy was graded (WCG) according to the National Cancer Institute (NCI) Common Toxicity Criteria, version 2.0. The patients were categorized into two groups according to their WCG: patients with WCG_{0-1} (group 1) and patients with WCG_{2-3} (group 2). The daily UV and BW changes, compared with the baseline BW, on days 2–5 of the chemotherapy regimens were noted, and differences in the averages of these measures between groups 1 and 2 were evaluated using repeated measures analyses of variance. Correlations between daily UV and BW changes were assessed using scatter diagrams and Pearson correlation coefficients.

The daily UV on days 1–5 and the maximum BW loss during days 1–5 of the first chemotherapy course were calculated for each patient. These parameters, the pretreatment parameters, the use of furosemide, and their associations with the two group categories were evaluated using χ-tests for categorical variables, Mann–Whitney tests for continuous variables, and logistic regression analyses for both types of variables. The total furosemide dose was calculated using the following formula:[9]

$$\text{total furosemide dose (mg)} = \text{intravenous dose (mg)} + 0.65 \times \text{oral dose (mg)}.$$

The Dr SPSS II 11.0 for Windows software package (SPSS Japan, Tokyo, Japan) was used for the statistical analyses.

Results

Between November 2000 and May 2006, 427 patients met the four inclusion criteria. Of these, six patients were excluded because their pretreatment serum creatinine levels were elevated, and four patients were excluded because no data on their daily UV or BW were available. Thus, a total of 417 patients were analyzed in the present study. The subjects comprised 327 men and 90 women, with a median age of 59 years (range 18–78 years) (Table 1). Non-small cell lung cancer was the most common tumor type, noted in 338 patients, followed by small cell lung cancer in 71 patients, thymic cancer in four patients, malignant mesothelioma in three patients, and tracheal cancer in one patient. Thirty-two patients with stage I–II diseases received chemotherapy as an adjuvant therapy after surgery. The remaining 385 patients with stage III–IV diseases or postoperative recurrent diseases received chemotherapy for the treatment of locally advanced or metastatic diseases.

All of the patients received cisplatin at a dose of 80 mg/m^2 in combination with other agents. The chemotherapy regimens were cisplatin and vinorelbine (n = 200), cisplatin and etoposide (n = 77), cisplatin, vindesine and mitomycin (n = 48), cisplatin and irinotecan (n = 41), cisplatin and gemcitabine (n = 41), and cisplatin and docetaxel (n = 10). The WCG was evaluated in all of the patients, with 390 patients categorized into group 1 and 27 patients categorized into group 2.

The average daily UV during days 1–5 of the chemotherapy regimens showed that the UV on day 1 did not differ between groups 1 and 2, but the daily UV on days 2–5 in group 2 were lower than those in group 1 (Fig. 1A, P = 0.042). The average changes in BW on days 2–5 showed that patients gained BW on days 2–3 and lost BW on days 4–5 (Fig. 1B). The line plotting the changes in BW in group 2 was always below that for group 1 (P = 0.036). Thus, the patients in group 2 retained less water than the patients in group 1. Furthermore, the patients in group 2 may have developed dehydration on day 5, as their average BW dropped to below the baseline level (Fig. 1B). Scatter diagrams comparing the average UV on days 1–2 and the BW change on day 3, and the average UV on days 1–4 and the BW change on day 5 showed no correlation between the UV and BW changes (data not shown), suggesting that the reduction in fluid intake may have caused the BW loss.

The development of renal toxicity was associated with some patient demographics. The percentage of women was higher in group 2 than in group 1 (11.1 *vs* 5.2%, P = 0.04). The median age of the patients in group 1 was 59 years (range 18–77 years), whereas that for group 2 was 65 years (range 38–74 years) (P = 0.041). None of the pretreatment chemistry parameters differed between the groups (Table 1). The frequency of renal toxicity did not differ according to chemotherapy regimen but was associated with a decreased average daily UV during days

© 2007 Japanese Cancer Association

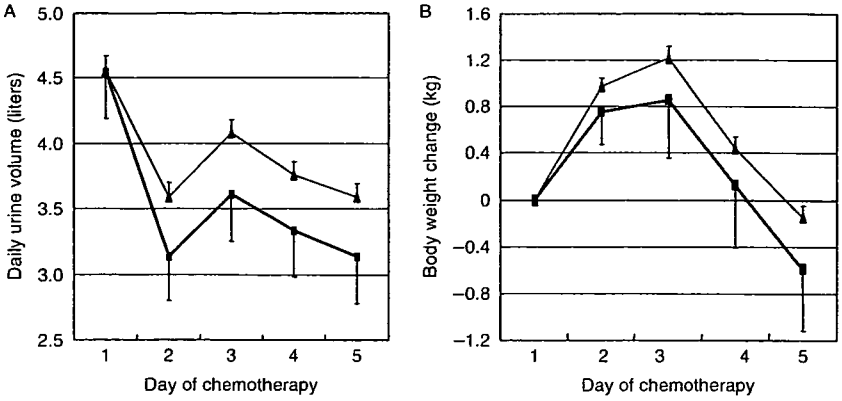

Fig. 1. (A) Average daily urine volumes during days 1–5 of chemotherapy. The differences were statistically significant ($P = 0.042$, repeated measures analysis of variance). (B) Average bodyweight changes on days 1–5 of chemotherapy. The differences were statistically significant ($P = 0.036$, repeated measures analysis of variance). Thin line with closed triangles: group 1, patients with a worst creatinine grade of 0–1 ($n = 390$); thick line with closed squares: group 2, patients with a worst creatinine grade of 2–3 ($n = 27$). Error bars show the 95% confidence intervals.

Table 2. Treatment-related parameters and groups categorized according to worst creatinine grade

		Group 1 ($n = 390$)		Group 2 ($n = 27$)		*P*-value
		n	%	*n*	%	
Agents combined with cisplatin	Vinorelbine	184	92.0	16	8.0	0.83
	Etoposide	74	96.1	3	3.9	
	Vindesine + mitomycin	45	93.8	3	6.2	
	Gemcitabine	39	95.1	2	4.9	
	Irinotecan	39	95.1	2	4.9	
	Docetaxel	9	90.0	1	10.0	
Average daily urine volume (mL)[†]	Median	3902	(Range 2058–6680)	3600	(Range 1700–5020)	0.021
	≤3000	41	87.2	6	12.8	0.054
	3001–4000	185	92.5	15	7.5	
	≥4001	164	96.5	6	3.5	
Maximum bodyweight loss (kg)[‡]	Median	0.2	(Range 0–3.9)	0.4	(Range 0–4.6)	0.11
	0	172	95.0	9	5.0	0.006
	0.1–2.0	201	93.9	13	6.1	
	≥2.1	17	77.3	5	22.7	
Total furosemide dose[§]	Median	0	(Range 0–160)	26	(Range 0–360)	0.024
	0	201	95.2	10	4.7	0.015
	1–30	87	94.6	5	5.4	
	31–60	70	93.3	5	6.7	
	61–90	11	91.7	1	8.3	
	≥91	21	77.8	6	22.2	

[†]The average daily urine volume on days 1–5 of chemotherapy. [‡]Maximum body weight loss during days 1–5 of chemotherapy. [§]Total furosemide dose (mg) = intravenous dose (mg) + 0.65 × oral dose (mg). Groups 1 and 2 were patients with worst creatinine grades of 0–1 and 2–3, respectively.

1–5 of the chemotherapy regimens (Table 2). In addition, only 5–6% of the patients with a maximum BW loss of 2 kg or less were classified as WCG_{2-3}, whereas 23% of the patients with a maximum BW loss of more than 2 kg were classified as WCG_{2-3} ($P = 0.006$). Furosemide was administered to 206 of the 417 patients (49.4%). Of these patients, 198 did not complain of any symptoms whereas eight developed mild edema in the lower extremities or face, which disappeared after a few days. The difference in the frequencies of renal toxicity among patients who received furosemide and those who did not (8.3 *vs* 4.7%, respectively; $P = 0.14$) was not large enough to be statistically significant. Administration route (intravenous or oral), day of use (day 1, day 2 or days 3–8), or BW gain just before use of furosemide (0–1.4, 1.5–2.9 or ≥3.0 kg) did not influence the frequency of renal toxicity. The total dose of furosemide, however, differed between groups 1 and 2 (median, 0 mg; range, 0–160 mg *vs* median, 26 mg; range, 0–360 mg, respectively; $P = 0.024$). In particular, 22% of the patients who received more than 90 mg of furosemide were classified as WCG_{2-3} (Table 2).

A multivariate analysis showed that the maximum BW loss (odds ratio, 1.77; 95% confidence interval, 1.08–2.90) and the total furosemide dose (odds ratio, 1.21; 95% confidence interval, 1.11–1.33) were significantly associated with the WCG_{2-3} category. Associations with sex and the daily UV were marginally significant (Table 3).

Discussion

The present study showed that the maximum BW loss during days 1–5 of chemotherapy was associated with the development of cisplatin renal toxicity. In particular, 23% of patients with a maximum BW loss of more than 2 kg were classified as WCG_{2-3}. Because dehydration amounting to as little as a 2% loss in BW results in impaired physiological and performance responses,[10] the BW loss and dehydration observed in the present study may be enough to aggravate cisplatin nephrotoxicity. No correlation was noted between the UV and BW changes, suggesting that the dehydration was attributable to a reduced oral intake by patients as a result of cisplatin-induced emesis. BW measurements are

doi: 10.1111/j.1349-7006.2007.00532.x
© 2007 Japanese Cancer Association